Acta Cryst. (1999). B**55**, 767–787

X-ray and neutron diffraction study of benzoylacetone in the temperature range 8–300 K: comparison with other *cis*-enol molecules

Frank H. Herbstein,[a]* Bo Brummerstedt Iversen,[b] Moshe Kapon,[a] Finn Krebs Larsen,[b] Georg Kent Hellerup Madsen[b] and George M. Reisner[a]

[a]*Department of Chemistry, Technion, Israel Institute of Technology, Haifa 32000, Israel, and* [b]*Department of Chemistry, University of Aarhus, DK-8000 Århus C, Denmark. E-mail: chr03fh@tx.technion.ac.il; kre@kemi.aau.dk*

(*Received 17 October 1998; accepted 30 March 1999*)

We dedicate this paper to Professor J. D. Dunitz F.R.S. on the occasion of his 75th birthday.

Abstract

The crystal structure of benzoylacetone (1-phenyl-1,3-butanedione, $C_{10}H_{10}O_2$; $P2_1/c$, Z = 4) has been determined at 300, 160 (both Mo $K\alpha$ X-ray diffraction, XRD), 20 (λ = 1.012 Å neutron diffraction, ND) and 8 K (Ag $K\alpha$ XRD), to which should be added earlier structure determinations at 300 (Mo $K\alpha$ XRD and ND, λ = 0.983 Å) and 143 K (Mo $K\alpha$ XRD). Cell dimensions have been measured over the temperature range 8–300 K; a first- or second-order phase change does not occur within this range. The atomic displacement parameters have been analyzed using the thermal motion analysis program *THMA*11. The most marked change in the molecular structure is in the disposition of the methyl group, which has a librational amplitude of ~20° at 20 K and is rotationally disordered at 300 K. The lengths of the two C—O bonds in the *cis*-enol ring do not differ significantly, nor do those of the two C—C bonds, nor do these lengths change between 8 and 300 K. An ND difference synthesis (20 K) shows a single enol hydrogen trough (rather than two half H atoms), approximately centered between the O atoms; analogous results were obtained by XRD (8 K). It is inferred that the enol hydrogen is in a broad, flat-bottomed single-minimum potential well between the O atoms, with a libration amplitude of ~0.30 Å at 8 K. These results suggest that at 8 K the *cis*-enol ring in benzoylacetone has quasi-aromatic character, in agreement with the results of high-level *ab initio* calculations made for benzoylacetone [Schiøtt *et al.* (1998). *J. Am. Chem. Soc.* **120**, 12117–12124]. Application [in a related paper by Madsen *et al.* (1998). *J. Am. Chem. Soc.* **120**, 10040–10045] of multipolar analysis and topological methods to the charge density obtained from the combined lowest temperature X-ray and neutron data provides evidence for an intramolecular hydrogen bond with partly electrostatic and partly covalent character, and large *p*-delocalization in the *cis*-enol ring. This is in good agreement with what is expected from the observed bond lengths. Analysis of the total available (through the Cambridge Structural Database, CSD) population of *cis*-enol ring geometries confirms earlier reports of correlation between the degree of bond localization in the pairs of C—C and C—O bonds, but does not show the dependence of bond localization on d(O···O) that was reported earlier for a more restricted sample. It is suggested that the only reliable method of determining whether the enol hydrogen is found in a single or double potential well is by low-temperature X-ray or (preferably) neutron diffraction.

1. Introduction

Benzoylacetone (1-phenyl-1,3-butanedione – this *Chemical Abstracts* nomenclature is far removed from the actual structure) can be considered as a representative example of a chemically unsymmetrical (Scheme 1; R_1 = CH_3; R_2 = C_6H_5; R_3 = H), but geometrically symmetrical β-diketone enol; here 'geometrically symmetrical' is taken to mean that the two C—O and the two C—C bond lengths as found by crystal structure analysis do not differ significantly *within* the pairs. We have chosen to study the crystal and molecular structure of benzoylacetone in two separate, but related, contexts.

The first context concerns the capability of diffraction methods to discriminate between fine details of molecular structure. How is the equilibrium (1*c*) shown in Scheme 1 to be interpreted? One possibility is as between two separate tautomers (which are necessarily valence isomers), the value of the equilibrium constant depending on the nature of the substituents; this has been the traditional approach in considering the solution physical chemistry. These two tautomers may be superposed in the crystal (either statically or dynamically), with the resultant material appearing to be disordered (1*d*) if the time scale of the measurements is appropriate. As a corollary, such a disordered structure could become ordered on cooling or application of pressure. Alternatively, an apparently disordered structure could be a true resonance hybrid (1*e*) such as is found for benzene, with the valence isomers now

© 1999 International Union of Crystallography
Printed in Great Britain – all rights reserved

ISSN 0108-7681 © 1999

becoming canonical forms. These questions are not new – whether diffraction techniques are capable of distinguishing between the D_{6h} and D_{3h} structures of benzene has been considered by Ermer (1987) and the analogous problems encountered with tetra-*tert*-butyl-*s*-indacene and tetra-*tert*-butylcyclobutadiene by Dunitz, Krüger *et al.* (1988).

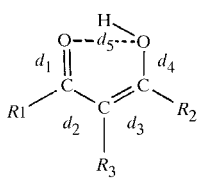

(1*a*) Triply-substituted *cis*-enol

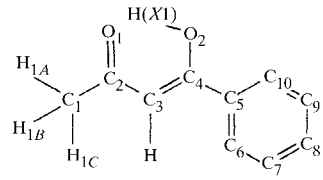

(1*b*) Benzoylacetone

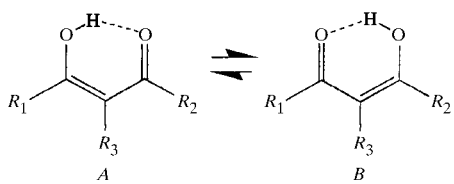

(1*c*) Hydrogen transfer between two tautomers *A* and *B*

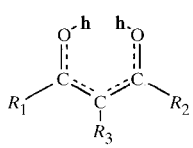

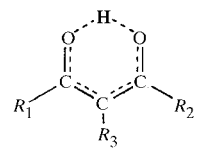

(1*d*) Static or dynamic disorder gives averaged structure for C, O and double-well potential for hydrogen; '**h**' represents half-hydrogen.

(1*e*) Ordered resonance structure with approximately centred enol hydrogen.

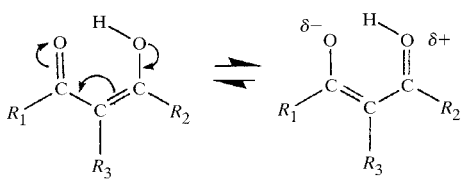

(1*f*), (1*g*) Charge redistribution according to the resonance-assisted hydrogen-bond model RAHB

In the second context we consider benzoylacetone as a simple example of intramolecular hydrogen bonding. Excellent summaries of earlier work have been given by Emsley (1984) (*The Composition, Structure and Hydrogen Bonding of the β-Diketones*) and by Hibbert & Emsley (1990) (*Hydrogen Bonding and Chemical Reactivity*), while it is fair to say that the subject has been transformed by the extensive contributions of Gastone Gilli and his school to the study of inter- and intramolecular hydrogen bonding (for a summary, see Gilli *et al.*, 1996; GFG96; more recent papers are Bertolasi *et al.*, 1996, 1997). Strong hydrogen bonding is often characterized as being charge-assisted (CAHB) and is found, for example, between an acid and its conjugated base or between a base and the protonated base. In CAHB systems the strong hydrogen bond is an effect of polarization of charge. A negatively charged acceptor strongly attracts the positive end of the bond dipole. Gilli *et al.* (1989; GBFB89) have proposed a resonance-assisted hydrogen bond model (RAHB; Scheme 1*f* and *g*) to account for the very short O—H···O (and N—H···O) distances observed in conjugated systems containing hydrogen bonds, resonance introducing partial charges with the appropriate signs to strengthen the hydrogen bond. Although the model was developed for both intra- and intermolecular hydrogen bonding, we consider here only the former situation (resonance shown in 1*e* of Scheme 1 and charge redistribution in 1*f* and 1*g*). The energy of the ring system will be lowered as the positive hydrogen nucleus moves towards the negative keto O atom. Thus, the RAHB model can be conceived as a feedback mechanism which maintains zero partial charge on the two opposite O atoms by neutralizing the increase in polarization due to resonance with a decrease caused by a shift in the proton position in the hydrogen bond. The RAHB model applied to *cis*-enol systems leads to a large degree of charge delocalization and symmetrization, π-electron delocalization being a crucial part of the RAHB concept. Despite the large number of crystal structures reported as a database for development of the RAHB concept (*e.g.* GBFB89; Bertolasi *et al.*, 1991, BGFG91), these are almost all room-temperature X-ray diffraction studies and the requirement for reliably locating the enol hydrogen – the combination of neutron diffraction and low temperatures – is lacking. This is regrettable as the definition of the location and behavior of the enol hydrogen is generally the crux of any structural study of *cis*-enols.

The present study of benzoylacetone covers the temperature range 8–300 K, with emphasis on neutron and X-ray diffraction studies at very low temperatures [20 (1) and 8.4 (4) K, respectively]. Our purpose is to consider how diffraction methods can be used to discriminate among the plethora of possibilities noted above (context 1) and how electron density studies, in the framework of the Bader (1990) approach (see also Stewart, 1991; Koritsanszky, 1996), can extend the RAHB concept (context 2). These results are given in two related papers. Here we report cell dimensions measured at intervals of 10–25° over the range 8–300 K and the crystal structures by XRD at 300, 160 (all Mo $K\alpha$) and 8.4 K (Ag $K\alpha$), and by ND (λ = 1.012 Å) at 20 K. We then integrate all the available results to derive the geometrical structure of the molecule and its dependence on temperature. Finally we extend the discussion to other *cis*-enols with intramolecular hydrogen bonding.

The present paper provides the crystallographic foundation for the related paper (Madsen *et al.*, 1998) in which the total electron density and deformation

distributions obtained from the 20 K ND and 8.4 K XRD measurements are analysed in order to provide a detailed picture of the bonding in benzoylacetone, with emphasis on the intramolecular *cis*-enol hydrogen bond. A topological analysis provides a direct comparison with results obtained for systems lacking conjugation. We emphasize that this study deals with benzoylacetone in particular and *cis*-enols in general, in the solid state, and that extension of our conclusions to fluid media needs separate justification.

2. Determination of the crystal structure of benzoylacetone

2.1. *Earlier work*

Earlier diffraction measurements (Semmingsen, 1972, XRD, 300 K, BZOYAC; Jones, 1976*b*, ND, 300 K, BZOYAC01; Winter *et al.*, 1979, XRD, 143 K, BZOYAC02) showed that benzoylacetone is in the *cis*-enol form, with the two pairs of C—O and C—C distances not significantly different (see Fig. 9 and summary of values in Table J – the large amount of deposited material is listed in Table 1, deposited tables being given 'letter' designations).† The enol hydrogen appears to be vibrating in a slightly asymmetric potential well, at least down to 143 K, while the methyl group appears to be rotationally disordered over two azimuths at room temperature, but is ordered at 143 K. We integrate these earlier results in our discussion.

2.2. *Present crystal structure analyses*

2.2.1. *Sample preparation*. Commercially available benzoylacetone crystals gave poor diffraction patterns and thus the compound was first purified by sublimation and then recrystallized from pentane. The XRD crystal was cut and rolled to a spherical shape (0.3 mm diameter) and then inserted into a capillary; a spherical absorption correction was applied. The ND data were corrected for absorption using a Gaussian grid integration, 4 along **a**, 16 along **b** and 6 along **c**.

2.2.2. *Cell dimensions as a function of temperature for benzoylacetone*. Cell dimensions were measured as a function of temperature (8–300 K) using the variable-temperature four-circle diffractometer at Aarhus (Henriksen *et al.*, 1986); 48 reflections were used as 24 Friedel pairs ($10 \leq 2\theta \leq 37.4^\circ$), with Mo $K\alpha$ radiation employed over 20–300 K and Ag $K\alpha$ at 8 K. Temperature stability was $\sim\pm1$ K and the standard uncertainties (s.u.s) of the measurements were $\sim$0.002 Å and 0.01°; these values refer to the precision of a particular set of measurements. Comparisons among values of different authors (or different experiments for the same author) suggest that the accuracy may well be '$\sim$0.02 Å and 0.1°' (*cf.* Taylor & Kennard, 1986). The measured values are given in Table A and are presented graphically in a number of figures. The graphs of a, b, c, β and V against

Table 1. *Details of deposited material*

Table	Abbreviated title	Reference
A	Cell dimensions as a function of temperature	Present work (Aarhus)
B	Information about data collection and structure refinement for 300 and 160 K analyses.	Present work (Haifa and Aarhus)
C	Coordinates; 300 K, XRD	Semmingsen (1972)
	300 K, ND	Jones, 1976*b*
	300 K, XRD	Present work (Haifa)
D	ADPs (U^{ij}), 300 K, XRD	Semmingsen (1972)
	300 K, ND	Jones (1976*b*)
	300 K, XRD	Present work (Haifa)
E	Coordinates; 160 K, XRD	Present work (Aarhus)
	143 K, XRD	Winter *et al.* (1979)
F	ADPs (U^{ij}); 160 K, XRD	Present work (Aarhus)
	143 K, XRD	Winter *et al.* (1979)
G	ADPs (U^{ij}); 20 K, ND	Present work (Aarhus)
H	ADPs (U^{ij}); 8.4 K, XRD	Present work (Aarhus)
I	Best planes at 8.4 K by XRD	Present work (Aarhus)
J	*cis*-Enol bond lengths at various temperatures	Present work
K	THMA; 300 K, XRD	Present work (Haifa)
L	THMA; 160 K, XRD	Present work (Aarhus)
M	THMA; 143 K, XRD (data of Winter *et al.*, 1979)	Present work (Haifa)
N	THMA; 20 K, ND	Present work (Aarhus)
O	THMA; 8.4 K, XRD	Present work (Aarhus)
P	Dimensions of *cis*-enol group in benzoylacetone as determined by various authors	Present work
Q	Geometrical values for *cis*-enol groups from the CSD	
R	NMR of benzoylacetone	
S	^{13}C chemical shifts in acetylacetone, benzoylacetone and dibenzoylmethane	

For THMA of 300 K ND ADPs (U^{ij}), see Jones (1976*b*). Material concerning 'other techniques which have been or could be used' has also been deposited.

† Supplementary data for this paper are available from the IUCr electronic archives (Reference: SH0126). Services for accessing these data are described at the back of the journal.

T all show distinct changes of slope at $T \simeq 220$ and 120 K (Fig. 1).

There is a remarkable similarity in the temperature dependence of b, c and V when compared with that of a in double-Y plots (Fig. 2). These diagrams show an unusual behavior – the crystal contracts in the same way in the three axial directions as the temperature is lowered. Usually (lower-symmetry) crystals have markedly anisotropic properties and this is also manifested in their thermal expansion. There is another unusual feature in that the graphs of dimension *versus* temperature (Fig. 1) approach their limiting values asymptotically only at temperatures below 20 K. The relative dimensions $X(T)/X(294)$ are also shown (Fig. 3) and have the same overall shape, although there are differences from one to the next (*e.g.* c falls by 1.5% between 294 and 8 K, whereas a falls by 3.0% over this temperature range). At first glance one would expect these effects, particularly the changes of slope, to herald a phase transition of some kind, but the diffraction patterns (which were carefully checked over the whole temperature range) do not show any abrupt changes in cell dimensions, or multiplication of cell volume or change in crystal symmetry. Thus, first- or second-order phase transitions do not occur between 300 and 8 K. Parallel measurements of specific heat would be helpful in interpreting these phenomena.

2.2.3. *Benzoylacetone crystal structure analyses*. Atomic numbering is shown in Scheme 1(*b*); Hazell's (1995) system of programs was used extensively. Experimental details of the 8.4 K XRD and 20 K ND measurements and refinements are given in Table 2. Details of the standard methods used by us for the 300 K (at Technion) and 160 K (at Aarhus) XRD analyses, and

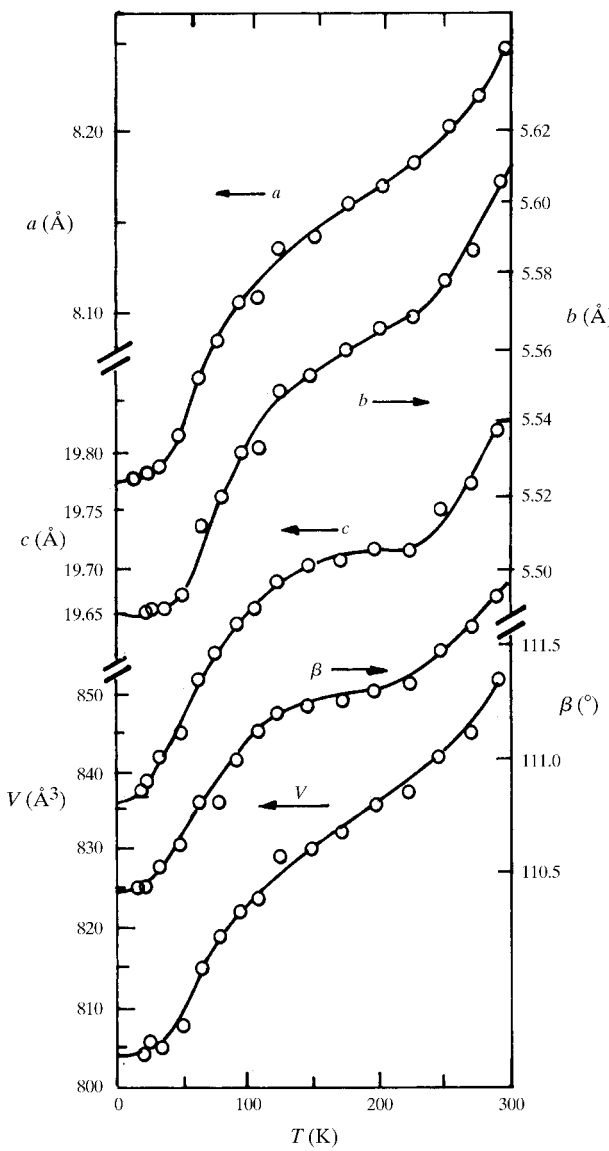

Fig. 1. Cell dimensions of benzoylacetone as a function of temperature for a, b, c, β and V. The lines joining the points serve only as a guide to the eye.

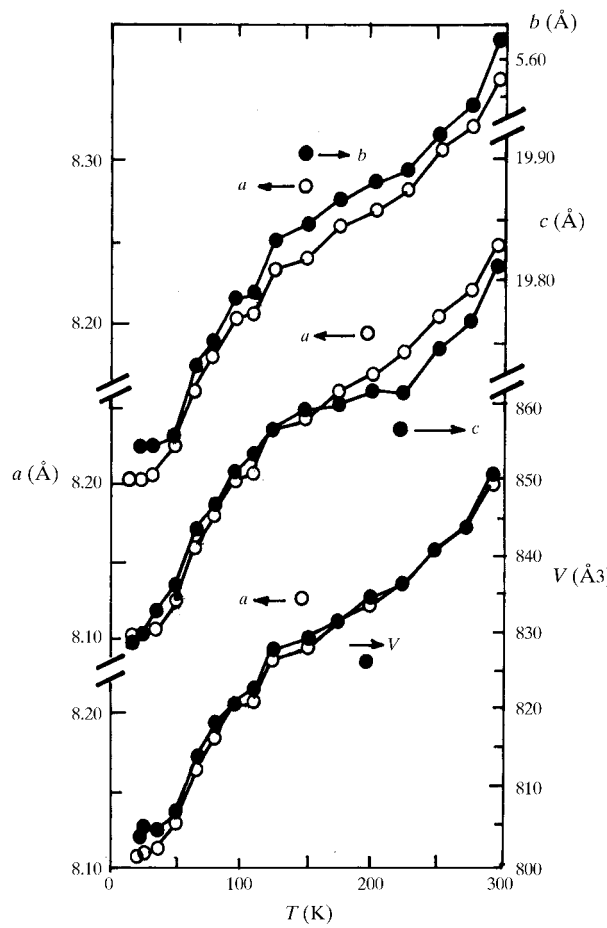

Fig. 2. Double Y plots of a *versus* the other cell dimensions for benzoylacetone, showing the parallelism in the changes. The lines are a guide to the eye.

Table 2. *Experimental details for XRD (8.4 K) and ND (20 K) measurements on benzoylacetone*

Both XRD and ND data were integrated using the program *COLL5N* (Lehmann & Larsen, 1974). The intensities were normalized to those of the standard reflections and corrected for absorption using a Gaussian integration approximation (Coppens *et al.*, 1965) with the system *KRYSTAL* (Hazell, 1995). The X-ray data were also corrected for Lorentz and polarization effects. Equivalent reflections were averaged using the program *SORTAV* (Blessing, 1989).

	X-ray	Neutron
Crystal data		
Chemical formula	$C_{10}H_{10}O_2$	$C_{10}H_{10}O_2$
Chemical formula weight	162.188	162.188
Crystal class	Monoclinic	Monoclinic
Space group	$P2_1/c$	$P2_1/c$†
a (Å)	8.006 (3)	8.027 (7)
b (Å)	5.482 (3)	5.483 (2)
c (Å)	19.444 (8)	19.478 (13)
β (°)	110.46 (3)	110.42 (5)
V (Å^3)	799.5 (5)	803.4 (6)
Z	4	4
D_x (Mg m^{-3})	1.350	1.341
Radiation type	Ag $K\alpha$	Neutron
Wavelength (Å)	0.5616	1.012 [Be (002) monchromator]
No. of reflections for cell parameters	91	50
θ range (°)	13.6–22.8	8.1–43.8
μ (mm^{-1})	0.0557	0.1993‡
Temperature (K) for cell parameters	20 (1)	20 (1)
Temperature (K) for data collection	8.4 (4) (cooling with CS202 DISPLEX He refrigerator)	20 (1) (cooling with CS201 DISPLEX He refrigerator)
Crystal form	Spherical	Prism
Crystal radius size (mm)	0.3	6 × 2.8 × 1.2
Crystal morphology (mm)	Colorless spherical crystal of 0.3 mm diameter	Colorless crystal bounded by ±[100] 1.2, ±[010] 6.0, ±[001] 2.8
Data collection		
Diffractometer	Type 512 Huber at Chemistry Department, Aarhus University (Henriksen *et al.*, 1986)	Type 512 Huber; beamline TAS2 at reactor DR3 at Risø National Laboratory
Data collection method	$2\theta/\omega$ scans	$2\theta/\omega$ scans
Duration of measurements (weeks)	5	6
Absorption correction	Gaussian (Frisch *et al.*, 1995)	Gaussian (Frisch *et al.*, 1995)
T_{min}	0.972	0.555
T_{max}	0.973	0.737
No. of measured reflections	10 494	2722
No. of independent reflections	2862	1597
No. of observed reflections	2013	1236
Criterion for observed reflections	$I > 2\sigma(I)$	$I > 2\sigma(I)$
R_{int}	0.024	0.023
θ_{max} (°)	25	45.19
Range of h, k, l	$-9 \rightarrow h \rightarrow 12$ $-8 \rightarrow k \rightarrow 8$ $-29 \rightarrow l \rightarrow 26$	$-11 \rightarrow h \rightarrow 10$ $-1 \rightarrow k \rightarrow 7$ $-6 \rightarrow l \rightarrow 27$
No. of standard reflections	3 ($0\bar{1}1$, 004, 800)	2 ($20\bar{4}$, $15\bar{2}$)
Frequency of standard reflections	Every 50 reflections	Every 60 reflections
Intensity decay (%)	3	0
Refinement		
Refinement on	F^2	F^2
$R[F^2>2\sigma(F^2)]$	0.0256	0.0516
$wR(F^2)$	0.0231	0.0500
S	0.900	2.250
No. of reflections used in refinement	2013	1236
No. of parameters used	307	219
Obs/par	6.55	5.64
H-atom treatment	H-atom parameters not refined	All H-atom parameters refined
Weighting scheme	$w = 1/[\sigma^2]$	$w = 1/[\sigma^2]$
$(\Delta/\sigma)_{max}$	0.06	0.01

Table 2 (*cont.*)

	X-ray	Neutron
$\Delta\rho_{max}$ (e Å^{-3})	0.146	0.044
$\Delta\rho_{min}$ (e Å^{-3})	−0.126	−0.040
Extinction method	None	XD§
Extinction coefficient	0	0.102 (4)
Source of atomic scattering factors	Clementi & Roetti (1974)	Sears (1992)

† A total of 309 space-group forbidden reflections, evenly distributed through reciprocal space, were measured. Inspection of their profiles convinced us that those few showing significant intensity were examples of multiple scattering (Le Page & Gabe, 1979) and that there was no justification for a change in space group. The average intensity of the space-group forbidden reflections was subtracted from all intensities and the same amount added to the variance of the measured intensities. ‡ A Gaussian integration approximation was used (Coppens *et al.*, 1965). Contributions from incoherent scattering (especially for the H atoms) were included (Howard *et al.*, 1989). § See Becker & Coppens (1974). An isotropic extinction model based on type 1 extinction and a Lorentzian distribution of mosaic blocks was included in the refinements [parameter 0.102 (4), which corresponds to a mosaic spread of 57 s of arc]. The presence of anisotropic extinction could not be tested because our measurements were not evenly distributed over reciprocal space. Ten reflections showed more than 10% extinction, three more than 15% and the worst case was $\bar{2}04$ with 30% extinction.

of the results obtained, which do not differ significantly from those in the earlier studies noted above, have been deposited, as have the atomic parameters for all the available analyses, except for the 20 (ND) and 8.4 K (XRD) coordinates given in Tables 3 and 4.

2.2.4. *Refinements based on 20 K ND and 8.4 K XRD measurements*. The ND data were refined by standard methods. The X-ray data were fitted to the aspherical atom formalism developed by Stewart (1973) and Hansen & Coppens (1978). The multipole refinement of the X-ray data was carried out using the program *XD* (Koritsanszky *et al.*, 1995). Details are given in the related paper.

2.3. *Comparison of various refinements*

Apart from a few exceptions, the three independent sets of 300 K atomic coordinates do not differ significantly; the s.u.s are all similar for non-H atoms, but XRD s.u.s for hydrogen are 3–4 times larger than those obtained by ND. The atomic displacement parameters (ADPs, U^{ij}) also agree well. However, one notes some *curiosa*; for example, Semmingsen's U^{33} values have s.u.s which appear to be perhaps ten times too large, while the converse applies to the s.u.s of his U^{12} values. There are also some differences in signs of cross-terms, which could be due to typographical errors. Our 160 K U^{ij} values are systematically 20–50% higher than those of Winter *et al.* (1979) at 143 K, although the trends are similar.† The s.u.s of ND coordinates for non-H atoms are about twice as large as those from comparable XRD analyses, while those for hydrogen are about one-third. The ND U^{ij} values for hydrogen at 20 K are about three times as large as those found for non-H atoms, either by XRD or ND. The $u(U^{ij})$ values for the non-H atoms determined by ND are about three times as large as those from XRD; the ND $u(U^{ij})$ values for H atoms are approximately 5–10 times as large as those for non-H atoms by XRD. We conclude that the most precise parameters (coordinates and ADPs) for non-H atoms are from XRD and for H atoms from ND. However, the hydrogen parameters are appreciably less precise than those of non-H atoms.

† A possible explanation, which would also fit Winter's cell dimension values (Table A), is that Winter's measurements were made at ∼100 K and not at 143 K. This would also improve the fit in Figs. 5, 6 and 7. Owing to the uncertainties, we have not changed the temperature from 143 K.

3. Crystal structure of benzoylacetone

3.1. *Arrangement of the molecules in the crystal*

An *ORTEP* (Johnson, 1976) stereodiagram of the crystal structure is shown in Fig. 4. The molecules are arranged across centers of symmetry, with O2 and O2′ separated by 3.049 (2) Å; analysis given in the related paper did not show a bond critical point between these

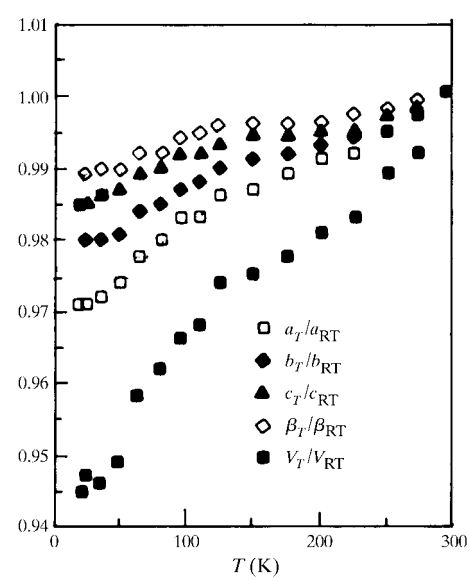

Fig. 3. Relative reduction in cell dimensions for benzoylacetone as a function of temperature, expressed as X_T/X_{RT}.

Table 3. *Positional parameters and U_{eq} at 8.4 K from XRD for benzoylacetone*

The values of U_{eq} (units of 10^{-4} Å^2) were calculated following Fischer & Tillmanns (1988) and their s.u.s following the isotropic and orthic approximation of Schomaker & Marsh (1983).

$$U_{eq} = (1/3)\Sigma_i\Sigma_j U^{ij} a^i a^j \mathbf{a}_i.\mathbf{a}_j.$$

	x	y	z	U_{eq}
O(1)	0.2432 (2)	0.3076 (3)	−0.0417 (1)	96 (5)
O(2)	0.4922 (2)	0.1317 (3)	0.0637 (1)	94 (6)
C(1)	0.1234 (2)	0.7008 (2)	−0.0363 (1)	102 (6)
C(2)	0.2507 (1)	0.4985 (2)	−0.0023 (1)	80 (6)
C(3)	0.3740 (2)	0.5199 (2)	0.0697 (1)	82 (6)
C(4)	0.4924 (1)	0.3281 (2)	0.1006 (1)	69 (6)
C(5)	0.6223 (1)	0.3358 (2)	0.1766 (1)	64 (5)
C(6)	0.6232 (1)	0.5266 (2)	0.2247 (1)	73 (5)
C(7)	0.7462 (1)	0.5262 (2)	0.2960 (1)	82 (5)
C(8)	0.8693 (2)	0.3368 (2)	0.3201 (1)	81 (6)
C(9)	0.8688 (1)	0.1466 (2)	0.2725 (1)	78 (5)
C(10)	0.7455 (1)	0.1444 (2)	0.2012 (1)	74 (5)

Table 4. *Positional parameters and U_{eq} for benzoylacetone, neutron study at 20 K*

The values of U_{eq} (units of 10^{-4} Å^2) were calculated following Fischer & Tillmanns (1988) and their s.u.s following the isotropic and orthic approximation of Schomaker & Marsh (1983).

$$U_{eq} = (1/3)\Sigma_i\Sigma_j U^{ij} a^i a^j \mathbf{a}_i.\mathbf{a}_j.$$

	x	y	z	U_{eq}
O(1)	0.2430 (3)	0.3084 (5)	−0.0416 (1)	129 (16)
O(2)	0.4920 (4)	0.1328 (5)	0.0635 (2)	128 (16)
C(1)	0.1230 (3)	0.7009 (4)	−0.0365 (1)	123 (14)
C(2)	0.2508 (3)	0.4990 (4)	−0.0023 (1)	102 (12)
C(3)	0.3743 (3)	0.5201 (4)	0.0698 (1)	101 (13)
C(4)	0.4923 (3)	0.3278 (4)	0.1007 (1)	93 (12)
C(5)	0.6226 (3)	0.3355 (4)	0.1765 (1)	88 (13)
C(6)	0.6231 (3)	0.5268 (4)	0.2245 (1)	103 (13)
C(7)	0.7466 (3)	0.5258 (4)	0.2962 (1)	105 (13)
C(8)	0.8688 (3)	0.3375 (4)	0.3200 (1)	98 (14)
C(9)	0.8690 (3)	0.1459 (4)	0.2724 (1)	111 (14)
C(10)	0.7455 (3)	0.1444 (4)	0.2012 (1)	103 (13)
H(1*A*)	0.1043 (11)	0.8211 (14)	0.0030 (4)	285 (33)
H(1*B*)	−0.0030 (9)	0.6301 (12)	−0.0694 (4)	249 (30)
H(1*C*)	0.1719 (9)	0.8054 (13)	−0.0705 (5)	258 (33)
H(3)	0.3782 (7)	0.6871 (10)	0.0992 (3)	249 (30)
H(6)	0.5282 (7)	0.6738 (9)	0.2073 (3)	267 (29)
H(7)	0.7453 (7)	0.6751 (9)	0.3328 (3)	265 (32)
H(8)	0.9666 (7)	0.3372 (10)	0.3755 (3)	679 (57)
H(9)	0.9658 (7)	−0.0013 (9)	0.2906 (3)	536 (50)
H(10)	0.7436 (7)	−0.0034 (10)	0.1641 (3)	717 (60)
H(*X*1)	0.3764 (19)	0.1768 (12)	0.0028 (5)	576 (62)

two atoms and so we conclude that this is not a weak hydrogen bond. The two centrosymmetrically related molecules are not coplanar, but have a stepped arrangement with an offset of 1.08 Å between their enol-group planes. The overall molecular arrangement does not vary with temperature. It seems unlikely that intermolecular interactions could significantly affect the geometry of the *cis*-enol group.

3.2. *Geometrical structure of the benzoylacetone molecule*

The benzoylacetone molecule as a whole deviates slightly from planarity, but the phenyl and enol groups are separately planar and are inclined to one another by an angle of 6.4° at 8 K (Table I); this angle (calculated for all the available sets of coordinates) varies by less than 0.2° over the temperature range investigated (we find 6.2° at 300 K). As the torsion angle O2—C4—C5—C10 is 5.7°, it is clear that the major contribution to the non-planarity of the molecule as a whole is from the torsion about the C4—C5 bond. Bond lengths have been reported over the temperature range 8–300 K; the values for the *cis*-enol ring are given in Table J. Bond lengths (corrected for thermal motion using *THMA*11; Trueblood, 1978; Dunitz, Schomaker & Trueblood, 1988) in the *cis*-enol ring have been plotted against T in Fig. 5. The molecular dimensions do not change appreciably with temperature (as has often been established, *e.g.* for naphthalene and anthracene; Brock & Dunitz, 1982, 1990), but it should be remembered that libration corrections at higher temperatures are subject to unknown (and possibly substantial) systematic errors.

The most precise values currently available for molecular dimensions involving C and O atoms are from the 8 K XRD measurements; those involving H atoms are from the 20 K ND measurements. The separate ND and XRD values are collected together in Table 5; corrections for anisotropic displacement at 8 K are small and hardly significant. One salient feature is a mean C—C bond length in the phenyl ring of 1.397 (5) Å, another (using the 20 K ND results) is the mean C—H length of 1.087 (5) Å; these are very close to standard values.

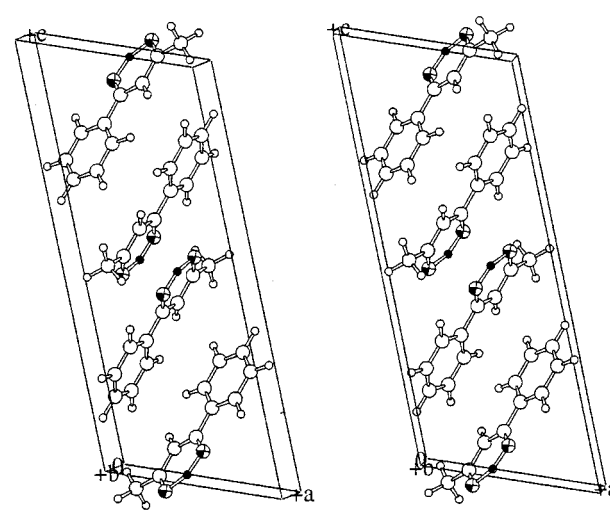

Fig. 4. *ORTEP* (Johnson, 1976) stereodiagram of the crystal structure of benzoylacetone; the O atoms and the enol hydrogen have been emphasized.

Table 5. *Benzoylacetone – molecular dimensions (Å, °)*

(*a*) Interatomic distances (Å) determined in the 20 K ND and the 8.4 K XRD studies. The small differences between ND and XRD $X-H$ distances are due to the use of fixed ND parameters for H atoms in the X-ray refinement; thus, s.u.s are omitted for XRD distances involving hydrogen.

	Neutron	X-ray
O(1)···O(2)	2.502 (4)	2.499 (2)
C(2)—O(1)	1.286 (4)	1.286 (2)
C(4)—O(2)	1.293 (4)	1.293 (2)
O(1)—H(*X*1)	1.329 (11)	1.325
O(2)—H(*X*1)	1.245 (11)	1.247
C(1)—C(2)	1.499 (4)	1.495 (2)
C(1)—H(1*A*)	1.064 (7)	1.060
C(1)—H(1*B*)	1.062 (8)	1.064
C(1)—H(1*C*)	1.051 (6)	1.050
C(2)—C(3)	1.414 (4)	1.408 (2)
C(3)—C(4)	1.405 (4)	1.402 (2)
C(3)—H(3)	1.076 (6)	1.076
C(4)—C(5)	1.483 (4)	1.481 (1)
C(5)—C(6)	1.406 (3)	1.402 (1)
C(5)—C(10)	1.404 (3)	1.405 (1)
C(6)—C(7)	1.402 (4)	1.391 (1)
C(7)—C(8)	1.387 (4)	1.395 (2)
C(8)—C(9)	1.404 (4)	1.395 (2)
C(9)—C(10)	1.394 (4)	1.392 (1)
C(6)—H(6)	1.079 (6)	1.079
C(7)—H(7)	1.090 (6)	1.087
C(8)—H(8)	1.091 (7)	1.086
C(9)—H(9)	1.090 (6)	1.092
C(10)—H(10)	1.085 (6)	1.081

(*b*) Bond angles (°) determined in the 20 K ND and the 8.4 K XRD studies. As the hydrogen parameters were not refined in the X-ray study, s.u.s are omitted for angles involving hydrogen.

	Neutron	X-ray
C(2)—O(1)—H(*X*1)	101.2 (4)	101.1
C(4)—O(2)—H(*X*1)	103.2 (4)	102.6
O(1)—H(*X*1)—O(2)	152.3 (6)	152.7
C(2)—C(1)—H(1*A*)	112.6 (5)	113.0
C(2)—C(1)—H(1*B*)	110.8 (4)	110.7
C(2)—C(1)—H(1*C*)	109.8 (4)	109.8
H(1*A*)—C(1)—H(1*B*)	108.7 (7)	108.4
H(1*A*)—C(1)—H(1*C*)	107.2 (7)	107.2
H(1*B*)—C(1)—H(1*C*)	107.7 (7)	107.5
O(1)—C(2)—C(1)	117.0 (3)	117.3 (2)
O(1)—C(2)—C(3)	122.1 (3)	122.0 (2)
C(1)—C(2)—C(3)	120.9 (2)	120.7 (2)
C(2)—C(3)—C(4)	119.7 (2)	119.8 (2)
C(2)—C(3)—H(3)	118.7 (4)	118.8
C(4)—C(3)—H(3)	121.5 (4)	121.3
O(2)—C(4)—C(3)	120.9 (3)	121.2 (2)
O(2)—C(4)—C(5)	116.4 (3)	116.2 (2)
C(3)—C(4)—C(5)	122.6 (2)	122.7 (2)
C(4)—C(5)—C(6)	121.5 (2)	121.7 (1)
C(4)—C(5)—C(10)	119.0 (2)	118.9 (1)
C(6)—C(5)—C(10)	119.5 (3)	119.4 (2)
C(5)—C(6)—C(7)	119.8 (3)	120.0 (1)
C(5)—C(6)—H(6)	120.9 (4)	120.6
C(7)—C(6)—H(6)	119.2 (4)	119.3
C(6)—C(7)—C(8)	120.4 (3)	120.5 (1)
C(6)—C(7)—H(7)	119.0 (4)	119.3
C(8)—C(7)—H(7)	120.6 (4)	120.2
C(7)—C(8)—C(9)	120.1 (3)	119.7 (2)
C(7)—C(8)—H(8)	120.7 (4)	120.7
C(9)—C(8)—H(8)	119.2 (4)	119.6

Table 5 (*cont.*)

	Neutron	X-ray
C(8)—C(9)—C(10)	119.9 (3)	120.3 (1)
C(8)—C(9)—H(9)	120.4 (4)	120.2
C(10)—C(9)—H(9)	119.7 (4)	119.5
C(5)—C(10)—C(9)	120.3 (2)	120.1 (1)
C(5)—C(10)—H(10)	119.1 (4)	119.2
C(9)—C(10)—H(10)	120.6 (4)	120.7

Other bond lengths agree well with those in the literature, but we shall not pursue this in detail as comparison of our 8 K values with 300 K values of other workers (or, at best, ∼100 K values) would be involved. Another feature is the closeness of the values of C2—O1 and C4—O2 [1.286 (2) and 1.293 (2) Å], and of C2—C3 and C3—C4 [1.408 (2) and 1.402 (2) Å]. The differences are $2.1u$ for the two pairs and thus are not significant, especially as Taylor & Kennard (1986) have shown that the s.u.s are probably underestimated. However, the values of d[O1—H(X1)] and d[O2—H(X1)] are 1.329 (11) and 1.245 (11) Å, and thus differ by $0.084/(2^{1/2} \times 0.011) = 5.4u$, which is significant; thus, there is ND evidence for a slight asymmetry in the positioning of the enol hydrogen.

3.3. *Analysis of thermal motion*

Standard methods (Schomaker & Trueblood, 1968; Trueblood, 1978; Dunitz, 1979; Dunitz, Maverick & Trueblood, 1988; Dunitz, Schomaker & Trueblood, 1988; computer program *THMA*11, version of 7 June, 1991; Trueblood, 1978; Dunitz, Schomaker & Trueblood, 1988) were applied to the non-hydrogen atomic coor-

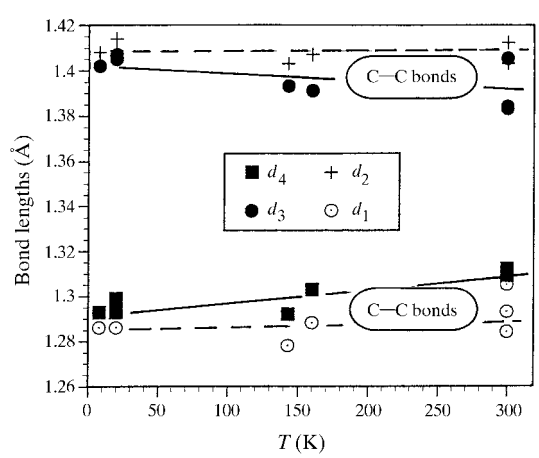

Fig. 5. Summary of present measurements of C—C and C—O bond lengths (Å; corrected for thermal motion) in the *cis*-enol ring of benzoylacetone as functions of T (K). $d_1 = d$(C2—O1), $d_4 = d$(C4—O2), $d_2 = d$(C2—C3) and $d_3 = d$(C3—C4). The lines through the points are guides to the eye. The s.u.s of the bond lengths are ∼0.005 Å, *i.e.* approximately half the vertical extensions of the points. A summary of earlier measurements is given in Table P (deposited).

Table 6. *Values of (eigenvalues)$^{1/2}$ of the librational (L_1, L_2, L_3; °) and translational (T_1, T_2, T_3; Å) tensors in the inertial frame (orthogonal axes X_1, X_2, X_3) at 300 (nominal), 160, 143, 20 (ND) and 8 K for benzoylacetone*

Values are for XRD measurements except as noted. The rigid-body parameters were obtained using only non-hydrogen U^{ij} values.

	300 K			160 K	143 K	20 K	8.4 K
	Haifa	Semmingsen	Jones (ND)	Aarhus	Winter	Aarhus (ND)	Aarhus
L_1	7.55	6.20	6.90	5.70	4.82	2.23	2.02
L_2	3.06	3.90	3.00	2.28	2.04	0.80	0.84
L_3	2.12	2.10	2.10	1.47	1.23	0.41	0.62
T_1	0.227	0.220	0.223	0.176	0.154	0.118	0.096
T_2	0.218	0.208	0.211	0.160	0.140	0.090	0.077
T_3	0.190	0.190	0.200	0.145	0.138	0.081	0.075

Table 7. *The angles between the librational (L_1, L_2, L_3) and inertial axes (X_1, X_2, X_3) and between the translational (T_1, T_2, T_3) and inertial axes at 160 and 8 K (XRD)*

The values for the librational axes are much the same at the other temperatures, while those for the translational axes vary widely.

	160 K			8 K		
	X_1	X_2	X_3	X_1	X_2	X_3
L_1	7.0	83.1	91.4	13.6	83.8	102.1
L_2	93.1	75.9	165.5	102.7	84.1	165.9
L_3	96.3	15.8	75.6	94.8	8.6	82.9
T_1	45.3	115.8	55.7	89.4	86.7	176.7
T_2	46.2	53.2	113.7	175.2	85.3	90.4
T_3	99.4	47.8	43.8	85.3	5.8	86.7

dinates and ADPs determined at the various temperatures to obtain the *square roots* of the eigenvalues of the librational and translational tensors in the inertial frame (Table 6), and the angles between the eigenvectors and molecular inertial axes (Table 7). The possible mutual libration of (assumed rigid) phenyl and enol groups about the C4—C5 bond was also considered. The libration amplitude is not larger than 1–2°, with appreciable s.u.s, and we have abandoned this parameter. In a separate calculation, using the ADPs from the 20 K ND results, we included the methyl group (with its H atoms) as a separate rigid body with freedom to librate about C2—C1; the RMS libration amplitude was found to be 19.7 (8)°.

In the harmonic approximation the mean-square librational and translational amplitudes are proportional to $h/(8\pi^2\mu\nu)\coth(h\nu/kT)$, where μ is the moment of inertia (for rotational motion) or reduced mass (for translational motion; Dunitz, Maverick & Trueblood, 1988; Dunitz, Schomaker & Trueblood, 1988). These values are plotted in Figs. 6 and 7 and reasonably good fits are obtained. The directions of the eigenvectors of the librational tensor with respect to the inertial frame (which, to a good approximation, does not change with temperature) differ by only a few degrees over the whole temperature range (Table 7). The largest amplitude of the librational tensor (L_1) lies approximately along the axis of least inertia X_1, while L_2 and L_3 lie between X_2 and X_3 (deposited Fig. A). As the ellipsoid of libration is rather anisotropic, its direction in crystal space is well defined. On the other hand, the translational ellipsoid is nearly isotropic, so it is difficult to define its direction and thus large differences are found among the directions of the eigenvectors of the translational tensor from the various structure analyses.

Similar (but more detailed) studies have been carried out for naphthalene over the range 80–240 K (Brock & Dunitz, 1982) and anthracene over the range 94–295 K (Brock & Dunitz, 1990). Only the naphthalene results will be considered here as there appear to be some problems with those for anthracene. The naphthalene experimental U^{ij} values were first corrected for internal molecular modes (not performed here for benzoylace-

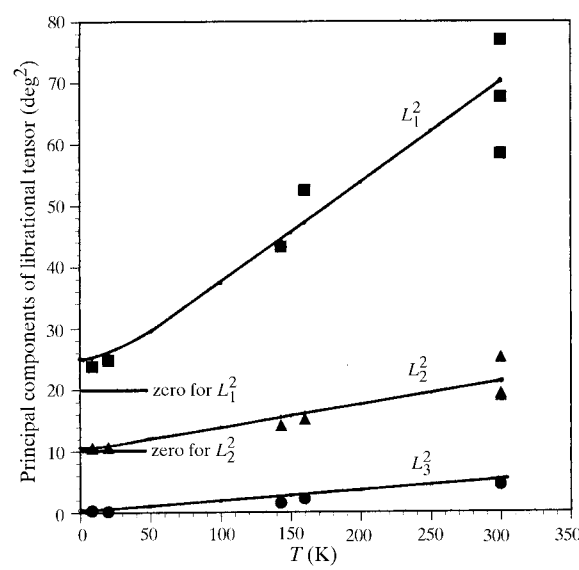

Fig. 6. Mean-square amplitudes of librational motion in the inertial frame plotted against T. For clarity, the L_1^2 and L_2^2 curves have been shifted up the vertical axis by 20 and 10 units, respectively, and the ordinate scales must be adjusted accordingly. The curves have the form 'a coth (b/T)', where the 'a's have been found from coth (b/T) $\Rightarrow 1$ as $T \Rightarrow 0$ and the 'b's from coth (b/T) $\Rightarrow T/b$ for small b/T.

tone) and then were analyzed in terms of a rigid-body model. The naphthalene 'L_i and T_i against T' plots showed a distinct curvature, whereas we find a linear dependence for benzoylacetone in the same temperature range. In broad terms the translational and librational motions in benzoylacetone are about twice as large as those in naphthalene. The thermal motion in L-alanine at 23 K (Destro *et al.*, 1988) can also be compared with that found here. Destro *et al.* (1988) reported that there were translational motions with root-mean square (r.m.s.) amplitudes of 0.06–0.07 Å in all three crystallographic directions, while a referee has added that the supplementary material to that paper gives r.m.s. libration amplitudes of 2.2, 1.6 and 1.5°. We find rather similar isotropic translations (r.m.s. values 0.08–0.10 Å) and librations (r.m.s. values of 2.0, 0.8 and 0.6°, with the largest value about the axis of least inertia; Table 6). Detailed comparisons of the various sets of values could be of interest, but we have not attempted to do this.

3.4. *Disposition of the methyl group*

The most striking effect of temperature on the molecular structure concerns the disposition of the methyl group, which takes up two azimuthal orientations at 300 K (ND results of Jones, 1976*b*). At 160 K we find only one orientation for the methyl group, although there is evidence for considerable libration of the methyl H atoms (Fig. 8*a*); this agrees with Winter's results. At 20 K the libration of the methyl H atoms is further reduced (Figs. 8*b–d*), but these atoms still have ADPs larger than those of *any* other atom in the molecule. Only ND measurements (300 and 20 K) give anisotropic ADPs for hydrogen; unfortunately, the 300 K results include U^{ij} values for all H atoms *except* those of the methyl group. At 20 K the methyl group is nearly 2/3 of the way to the staggered conformation with respect to the bond C2—O1, with τ(H1*B*—C1—C2—O1) = 38°. It is usual for a methyl group to be eclipsed with respect to a carbonyl bond. In the gas electron diffraction study of acetylacetone (Iijima *et al.*, 1987) the low barrier approximation was assumed, but the barrier was indeterminate between 0–20 kJ mol^{-1}; the methyl group was found to have a rotational angle of 30 ± 2° with respect to the heavy-atom plane, in reasonable agreement with our present value. The height of the potential barrier to methyl rotation can be estimated from the measured libration amplitude at 20 K [φ = 19.7 (8)°], using the classical Boltzmann averaging treatment of Maverick & Dunitz (1987); we obtain B = 0.6 kJ mol^{-1} K^{-1}. The changes of slope of the cell dimension–temperature

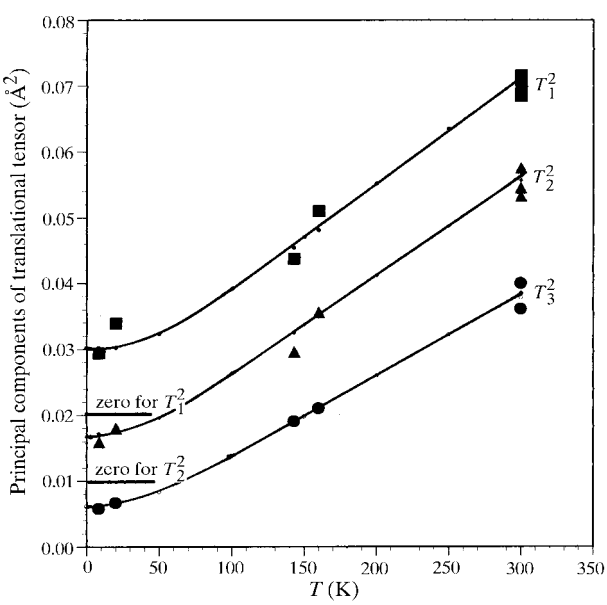

Fig. 7. Mean-square amplitudes of translational motion in the inertial frame plotted against T. For clarity, the T_1^2 and T_2^2 curves have been shifted up the vertical axis by 0.02 and 0.01 units, respectively, and the ordinate scales must be adjusted accordingly. The curves have the form 'a coth (b/T)', where the 'a's have been found from coth (b/T) ⇒ 1 as T ⇒ 0, and the 'b's from coth (b/T) ⇒ T/b for small b/T.

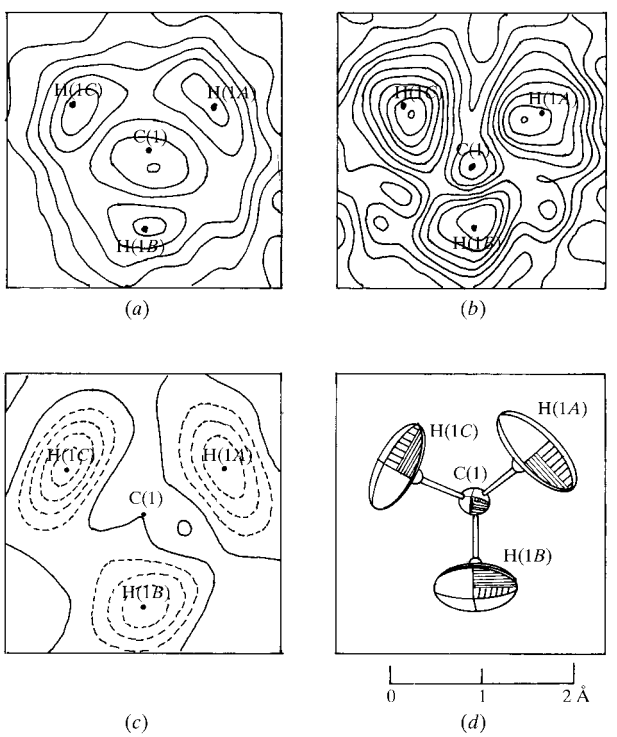

Fig. 8. Disposition of the methyl groups of benzoylacetone (*a*) at 160 K (all data); (*b*) at 20 K (sin θ/λ < 0.7 Å^{-1}); both XRD difference maps in the plane of the methyl H atoms, contour levels at 0.1 e Å^{-3}); (*c*) at 20 K (sin θ/λ < 0.7 Å^{-1}); ND difference map in the plane of the methyl H atoms, contour level 0.05 × 10^{-14} m Å^{-3}); (*d*) 50% probability ellipsoids for the methyl group viewed end-on; ND at 20 K; the open circles denote the 'bond critical points' (see related paper).

Table 8. *The r.m.s. values for the Δ_{AB} values (pm^2) for the bonded pairs of the phenyl and cis-enol groups, and for the remaining non-bonded pairs at the various temperatures of measurement*

T (K)	Bonded pairs		Non-bonded pairs
	Phenyl group	*cis*-Enol group	
8	6.7	7.0	12.4
20 (ND)	7.8	13.6	20.1
143	6.5	31.4	18.9
160	10.8	36.1	23.9
300 (Haifa)	27.0	55.3	37.4

graphs at ~220 and 120 K do not appear to be concerted with the gradual reduction in the libration amplitude of the methyl group as the temperature is reduced. We have noted above that the diffraction patterns do not show any evidence for the occurrence of a first- or second-order phase transition between 300 and 8 K. As there are no crystallographic restrictions on molecular symmetry (space group $P2_1/c$, $Z = 4$), modest changes in molecular arrangement or structure can occur without requiring changes in crystal symmetry. A similar situation occurs in citrinin, where the space group remains $P2_12_12_1$ ($Z = 4$) over the temperature range 19–300 K, despite a marked shift in the *para* $\Longleftrightarrow$ *ortho* equilibrium; the converse situation occurs in naphthazarin C (see §5).

3.5. *Hirshfeld rigidity analyses*

In a perfectly rigid molecule the mean-square displacement amplitudes resolved along the interatomic direction (MSDA values) for each atom of the pair A, B should be equal and thus their difference Δ_{AB} should be zero. Hirshfeld (1976) suggested that in practice the values of Δ_{AB} should not be greater than ~10 pm^2, otherwise the data were not of the highest quality or the molecule was not rigid. Hirshfeld added another condition not usually quoted or obeyed: that 'the refinement program allows explicitly for the bonding deformation'. Thus, strictly speaking, only our 20 K ND and 8 K XRD results may be analyzed by Hirshfeld's method. Methods of interpretation have been summarized by Dunitz, Schomaker & Trueblood (1988) and Dunitz, Maverick & Trueblood (1988); see also Chandrasekhar & Bürgi (1984). Δ_{AB} values for non-H atoms were determined from the various structure analyses using *THMA*11 applied to the U^{ij}s. Δ_{AB} values involving H atoms could be obtained only from the 20 K ND study. The validity of individual Δ_{AB} values can be tested by comparing values from appropriate pairs of independent analyses; the correlation coefficients R^2 for the pairs '8 K XRD and 20 K ND', and '143 K (Winter) and 160 K (Aarhus) XRD', are 0.05 and 0.40, respectively (plots deposited as Figs. B and C). Thus, a quantitative analysis based on the individual numerical values is not permissible, at least for the lowest temperatures for which the Δ_{AB} values are similar to their s.u.s. However, a qualititative discussion of overall trends is useful. It is usual to distinguish between bonded and non-bonded pairs of atoms; the Hirshfeld condition should apply strictly to bonded pairs, while deviations from it for non-bonded pairs are evidence for a lack of mutual rigidity of different parts of the molecule. The r.m.s. values for bonded and non-bonded atom pairs for the temperature range 8–300 K are given in Table 8. We use the phenyl ring for calibration and conclude that it is rigid until at least 160 K, but at higher

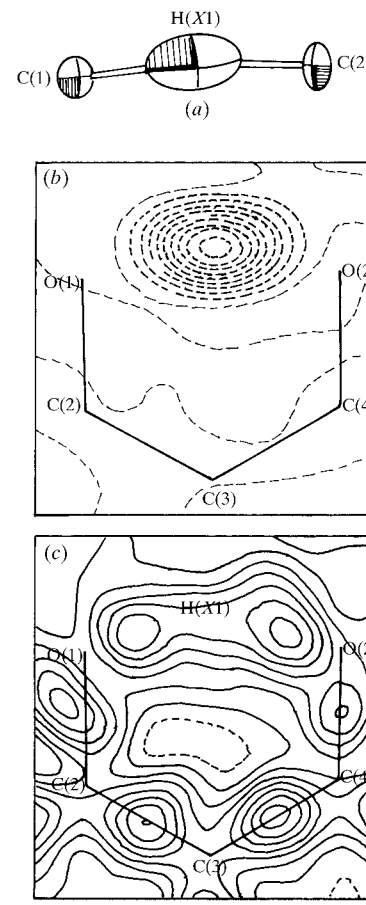

Fig. 9. (*a*) ADP 50% probability ellipsoids of the O···H···O group in benzoylacetone (20 K ND refinement), viewed in the plane of the *cis*-enol group; (*b*) difference map in the plane of the *cis*-enol group calculated from 20 K ND refinement, the enol hydrogen being omitted from the model. The contour interval is 0.05×10^{-14} m Å^{-3}; the dotted line is the zero contour and the broken lines negative contours. The scattering length of hydrogen is negative so the omitted enol hydrogen appears as a trough in the map; (*c*) difference map in the plane of the enol group from 8.4 K XRD data, calculated with the enol hydrogen included in the model. Solid lines are positive contours and broken lines negative contours (interval 0.1 e Å^{-3}). The peaks between oxygen and H(X1) nuclear positions are hydrogen bonding densities like the bonding deformation densities observed between carbon (and C and O) atoms.

temperatures the values are too large for reliable conclusions to be drawn about rigidity, disorder or deficiencies in the measurements. The *cis*-enol and phenyl groups show similar degrees of rigidity at 8 K, but their behaviors diverge at higher temperatures, even at 20 K.

The r.m.s. Δ_{AB} values for non-bonded atom pairs are rather similar to those of the bonded pairs; this situation is very different from that found for the orthorhombic polymorph of triphenylphosphine oxide at 100 K (Brock *et al.*, 1985; Dunitz, Schomaker & Trueblood, 1988) where 'the e.s.d.'s of the Δ values for the three rings is about 7 pm^2, and the r.m.s. Δ values for the three rings are 11, 6, and 8, respectively. Thus each ring is essentially rigid (ignoring any out-of-plane deformations, which would not be shown by this criterion). On the other hand, there is evidence of significant motions of the rings *relative* to each other ...the r.m.s. Δ values for blocks *AB* and *AC* are 4 or 5 times as large as those *within* each ring'. Thus, there is little mutual motion of phenyl and *cis*-enol rings in benzoylacetone, as already noted above in the discussion of the thermal motion analysis.† The values of Δ_{Y-C1}, where C1 is the methyl carbon and *Y* represents the other atoms, are rather larger than the other values at all temperatures, suggesting that the methyl group is not rigid with respect to the rest of the molecule.

From the 20 K ND study it was found that the numerical differences between MSDAs of bonded C and O atoms ranged from 0 to 20 pm^2; the corresponding values for bonded H atoms and C ranged from 81 to -11 pm^2 (only one negative value) for atoms of the rings and 48, 70 and 121 pm^2 for the three methyl H atoms. This is particularly conspicuous for the enol hydrogen where the Δ_{AB} values are 932 pm^2 (to O1) and 904 pm^2 (to O2); these values are discussed below. Thus, the H atoms have considerably larger vibration amplitudes than the C and O atoms.

3.6. *Search for disorder in the cis-enol ring*

How is the pairwise equality of the C—C and C—O bonds in the *cis*-enol ring to be interpreted? 'Standard' and 'unperturbed' values (Å) for bond lengths have been given by GBFB89 as follows: C—C [1.48; 1.454 (5)], C═C [1.33; 1.344 (3)], C—O [1.37; 1.353 (4)], C═O [1.20; 1.225 (3)]. The averages (using 'unperturbed' values) are 1.289 (C—O) and 1.399 Å (C—C); for simplicity we assume equal populations for the two (putative) valence isomers; the general case is given by Chandrasekhar & Bürgi (1984). Thus, a dynamic or static superposition of valence isomers could provide an explanation for the observed bond lengths. Such superpositioning gives pairs of C atoms (or O atoms) separated by ~0.1 Å. However, Ermer (1987) has argued, with regard to the analogous Kekulé valence isomers of benzene where the separation is ~0.06 Å, that 'this small separation is beyond the resolving power of a...diffraction experiment'. The resolution limit for two point atoms in a three-dimensional Fourier map is $0.71 d_{\min} \simeq 0.47$ Å (James, 1948); this value will be greater when more diffuse atoms are involved. Thus, a direct approach to checking whether disorder is present is not applicable. A possible alternative is *via* the Δ_{AB} values, as applied by Dunitz, Krüger *et al.* (1988) to two examples related to the present problem. In the first, tetra-*tert*-butyl-*s*-indacene, $\langle(\Delta_{AB})^2\rangle^{1/2} \simeq 7$ pm^2 for the bonded pairs of the indacene skeleton at 100 K and the molecule was inferred to be present as a stabilized transition state between two valence isomers. We quote 'if the observed structure were such a superposition [of valence isomers] the two sets of atomic positions could not differ from the averaged positions by more than 3 pm'. On the other hand, tetra-*tert*-butylcyclobutadiene shows ring 'bond lengths' that vary with temperature (1.464 and 1.483 Å at 300 K; 1.441 and 1.527 Å at 123 K) and the calculated (rigid body) tangential ADPs of the ring atoms are smaller than the observed values by ~40 pm^2, the discrepancy being ascribed to the presence of two rectangular-shaped valence isomers, disordered over two mutually perpendicular orientations and with displaced centers.

In benzoylacetone $\langle(\Delta_{AB})^2\rangle^{1/2}$ for the phenyl ring at 8 K is 7 pm^2 and the *cis*-enol group (excluding the enol hydrogen) has the similar value of 7 pm^2 (Table 8). Comparing observed ADPs with values calculated for a rigid-body model, we find the largest value of ΔU^{ij} (= $(|U^{ij}_{\rm calc} - U^{ij}_{\rm obs}|)$ is 23 pm^2 for the *cis*-enol ring and 9 pm^2 for the phenyl ring, with corresponding $\langle(\Delta U^{ij})^2\rangle^{1/2}$ values of 9.5 and 3.9 pm^2, respectively. Our $\langle(\Delta U^{ij})^2\rangle^{1/2}$ and $\langle(\Delta_{AB})^2\rangle^{1/2}$ values are about as large as the s.u.s of $U^{ij}_{\rm obs}$; the $\langle(\Delta_{AB})^2\rangle^{1/2}$ values are appreciably smaller than those for tetra-*tert*-butylcyclobutadiene and the coordination complexes considered by Chandrasekhar & Bürgi (1984), but similar to those for tetra-*tert*-butyl-*s*-indacene. Furthermore, unlike the situation in tetra-*tert*-butylcyclobutadiene, there are no systematic trends in the $\langle(\Delta_{AB})^2\rangle^{1/2}$ values. Based on these observations, we conclude that there is no evidence of disorder in the *cis*-enol ring of benzoylacetone at 8–20 K. At some undetermined temperature between 20 and 160 K, the *cis*-enol ring shows an increase in $\langle(\Delta_{AB})^2\rangle^{1/2}$; we have been unable to define the nature of this change in behavior. Our conclusions for benzoylacetone are opposite to those of Vila *et al.* (1992), which were partly based on our preliminary measurements.

It has recently been pointed out (Bürgi & Förtsch, 1997) that analysis of ADPs measured at a number of temperatures can give information about librational, translational and intramolecular motions not obtainable from measurements made at a single temperature;

† This is hardly surprising as both conclusions derive from analyses based on the same experimental measurements – the ADPs.

furthermore, certain types of disorder can be identified from the temperature evolution of the ADPs. The idea of using measurements of Bragg intensities made at a number of temperatures to demonstrate the presence of disorder is not new; for example, the method has been used to show that displacements from the sites of the average lattice occur in disordered f.c.c. and b.c.c. alloys owing to differences in the sizes of the component atoms (Huang, 1947; Herbstein *et al.*, 1956). It would be interesting to apply the Bürgi analysis, which is not yet in the public domain, to our present results. The situation in benzoylacetone is certainly more complicated than that in the alloys and one could hope to see differences in the behavior of atoms of the phenyl and *cis*-enol rings as the temperature is changed.

3.7. *Disposition of the enol hydrogen in benzoylacetone at very low temperatures*

The ND difference synthesis at 20 K [Fig. 9*b*; H(*X*1) omitted from F_{calc}] shows the enol hydrogen as a single broad trough elongated along the O···O vector. If we link two half-H atoms to the O atoms by bonds of 1.07 Å, then these half-H atoms will be separated by 0.46 Å. The single broad trough should be compared with the many examples of a pair of half-hydrogen peaks found in electron-density difference syntheses of *cis*-enol rings; acetylacetone (see later) provides one such example, while others are noted in Table 11. In our view the 20 K ND difference synthesis of benzoylacetone, in which no assumptions are made about the disposition of the enol hydrogen, provides the crucial evidence for the 'resonance' model of the *cis*-enol ring and against a model based on disordered superpositioning of two ordered structures. For convenience, we have added to Fig. 9 a diagram showing the vibrational ellipsoids of the O···H···O part of the molecule (Fig. 9*a*) and part of the deformation synthesis map calculated from the 8.4 K XRD data [Fig. 9*c*; H(*X*1) included in F_{calc}], which shows two bonding electron peaks at ∼0.6 Å from O1 and O2.

The $\Delta_{O1-H(X1)}$ and $\Delta_{O2-H(X1)}$ values are 932 and 904 pm^2, respectively. Averaging, we obtain that the hydrogen r.m.s. vibration amplitude in the O1···O2 potential well is ∼0.30 Å. Comparable values of vibration amplitudes have not been easy to find. Sequeira *et al.* (1968) have derived, from a room-temperature ND study, a broad single-minimum potential in potassium hydrogen diaspirinate (KHDASL01), where d(O···O) = 2.45 Å, with a value of 0.19 Å for the bond-parallel component of vibration. Schlemper *et al.* (1971) in their room-temperature ND study of 'a short, slightly asymmetrical, intramolecular hydrogen bond...[in] bis(2-amino-2-methyl-3-butanone oximato)Ni(II) chloride monohydrate' (AMBONC01) found a broad single-minimum potential with a value of 0.18 Å for the bond-parallel component of vibration. They suggest that 'the amplitude of hydrogen motion along the bond is somewhat greater than would be predicted from a harmonic oscillator model. The difference is too great to be accounted for by anharmonicities, and ...there must be an appreciable amount of static disorder in most hydrogen-bonded crystals... [here we] propose that local packing defects influence the potential enough so that the equilibrium position varies slightly from bond to bond throughout the crystal, thus giving rise to an apparent large vibration amplitude'. This interesting but iconoclastic idea would presumably have to be tested by single-crystal polarized IR spectroscopy.

4. Comparison with acetylacetone and 2-phenylmalonaldehyde enol

Acetylacetone is chemically very similar to benzoylacetone, but experiment shows that there are clear differences in structure. Although early gas electron diffraction (GED) results had suggested a structure both chemically and geometrically symmetrical, a later GED study showed localization of single and double bonds (Iijima *et al.*, 1987), in agreement with what had been found in the crystal structure analysis of the 9-ethyladenine-diphenylhydantoin-acetylacetone complex (Camerman *et al.*, 1983). The crystal structure of acetylacetone itself (m.p. 250 K) has been determined at 110 K by XRD (Boese *et al.*, 1998). The unit cell contains four molecules; the systematic absences give $Pn2_1a$ (a non-standard setting of $Pna2_1$) and *Pnma* as possible space groups. It seems unlikely (on the basis of examples and arguments given by Marsh, 1986) that meaningful refinement could be achieved in space group $Pn2_1a$; neutron diffraction with concentration on the weaker reflections could, perhaps, enhance the chances of success. However, Boese *et al.* (1998) were not able to carry out a satisfactory refinement in $Pn2_1a$. If *Pnma* is chosen (following Marsh's, 1986, recommendation†), then the molecule has a (real or apparent) mirror plane. The fact that two half-H atoms appear in the difference synthesis shows that the mirror symmetry is due to disorder and not to delocalization. Thus, we conclude, on the basis of the Iijima and Camerman results, that acetylacetone has a geometrically unsymmetrical *cis*-enol ring, without delocalization. The results of Boese *et al.* (1998) are compatible with this conclusion if disorder is assumed. The measured dimensions for acetylacetone are summarized in Table 9. It is not known whether the disorder in crystalline acetylacetone (presuming there is such) is dynamic or static; powder neutron diffraction shows a phase change of an as-yet undetermined nature below 110 K. It is important to note that acetylacetone is in the *cis*-enol form in both gas and solid states.

† 'In cases where diffraction data do not provide a clear choice between a centrosymmetric and a non-centrosymmetric space group, it is better to opt for the centrosymmetric description even though disorder may result.'

Table 9. *Summary of reported bond lengths (Å) for acetylacetone*

The distances are defined in the formula: d_5 [= d(O···O)].

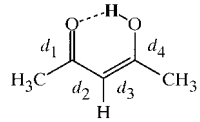

Reference	d_1	d_2	d_3	d_4	d_5	d(O–H)
(*a*) (ED)	1.243 (2)	1.430 (8)	1.382 (7)	1.319 (3)	2.512 (8)	1.049 (15)
(*b*) (XRD)	1.238 (10)	1.412 (10)	1.338 (10)	1.331 (10)	2.546 (10)	1.03 (9)
(*c*) (XRD)	1.292 (1)†	1.402 (1)†			2.546 (1)	0.88 (2)†
(*d*) Theory‡	1.259	1.452	1.376	1.338	2.549	1.004

(*a*) Iijima *et al.* (1987); (*b*) Camerman *et al.* (1983); acac in complex; (*c*) Boese *et al.* (1998; see text); at 110 K; (*d*) Dannenberg & Rios (1994). † Single values because of symmetry. ‡ At level MP2/95**.

2-Phenylmalonaldehyde (Scheme 1*a*, $R_1 = R_2 = H$, $R_3 = C_6H_5$) is an example of an enol which demonstrates the sensitivity of these systems. An NMR study (^1H, ^{13}C) has recently shown unequivocally that this compound is in the unsymmetric *cis*-enol conformation in solution, corresponding to the presence of two equilibrating tautomers (Perrin & Kim, 1998). However, in the solid state at 91 K the molecule is in the *trans*-enol configuration, with intermolecular, but no intramolecular, hydrogen bonding (Semmingsen, 1977).

5. Comparison with other multi-temperature structure analyses

Benzoylacetone shows changes of slope in the cell dimension–temperature graphs, together with a non-concerted gradual reduction in the libration amplitude of the methyl group as the temperature is reduced. There is no evidence for a first- or second-order phase transition between 300 and 8 K. Modest changes in molecular arrangement or structure can occur without requiring changes in space group. A similar situation occurs in citrinin, where the space group remains $P2_12_12_1$ ($Z = 4$) over the temperature range 300–19 K despite a marked shift in the *ortho* $\Longleftrightarrow$ *para* equilibrium (see §6).

Are there other examples of similar effects? Sodium 1-pyrrolidenecarbodithioate dihydrate, whose structure has been determined at 295, 150 and 27 K (Albertsson *et al.*, 1980; space group $P2_1/a$, $Z = 4$, at all three temperatures), is one. The five-membered pyrrolidinyl ring is in a disordered quasiplanar conformation at 295 and 150 K, but is ordered in a twist conformation at 27 K; thus, there is a change of conformation *without* a change of phase.

6. Comparison of benzoylacetone, citrinin and naphthazarin C

Our results can be usefully compared with those for citrinin and naphthazarin, which are chemically related to the *cis*-enols, but differ from them. The charge density in crystalline citrinin (Scheme 2; $C_{13}H_{14}O_5$; melts with decomposition at 452 K) has been studied by XRD at 240, 147 and 19 K (Destro & Marsh, 1984; Destro, 1991; Roversi *et al.*, 1996); the 19 K study was particularly detailed.† There has also been a ^{13}C, ^1H and ^{17}O NMR study of citrinin in the solid state and in aprotic and protic solvents (Poupko *et al.*, 1997); the protic solvents do not concern us here. Citrinin has two tautomeric forms, which impose valence isomerism; the *ortho* $\Longleftrightarrow$ *para* equilibrium constant is unity at 356 K, with the *o*-quinone form predominating above this temperature (if no other changes such as decomposition occur) and the *p*-quinonemethide form below. The NMR studies confirm the model obtained from XRD and show that the tautomerism is extremely fast on the NMR time scale (...'lower limit of 10^6 s^{-1} for the rate, but it could be (and probably is) several orders of magnitude faster'...). Despite the marked shift in the *ortho* $\Longleftrightarrow$ *para* equilibrium the space group remains $P2_12_12_1$ ($Z = 4$) over the temperature range 300–19 K and the molecular arrangement does not change. Our comparison is between benzoylacetone at 8.4 K and citrinin at 19 K. There are two keto–enol-like ring systems with short intramolecular O—H···O hydrogen bonds in the citrinin molecule. Although the two O···O distances in the citrinin molecule, 2.473 and 2.533 Å, are similar in length to the corresponding O···O distance of 2.499 Å in benzoylacetone, the bond lengths within the keto–enol rings are quite different in the two molecules. The two fused ring systems of citrinin have distinctly alternating bond lengths in contrast to benzoylacetone. Also, the H atoms in the O—H···O bonds of citrinin are located much more asymmetrically, linked to the enol O atoms with bond lengths of 0.974 (11) and 1.056 (10) Å, respectively. These values are close to average values for normal alcoholic and acidic protons by neutron

† The $(\sin\theta/\lambda)_{max}$ values for benzoylacetone (8.4 K) and citrinin (19 K) were 0.75 and 1.14 $Å^{-1}$, respectively.

diffraction. The topology of the enol ring charge density in the two systems is compared in the related paper.

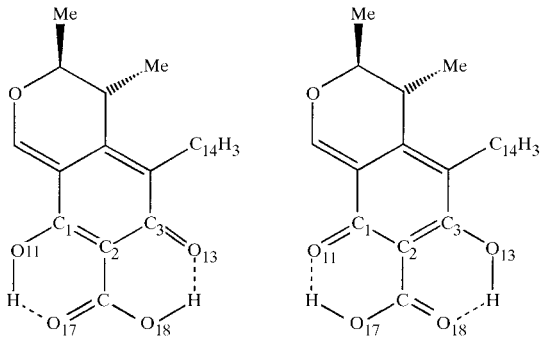

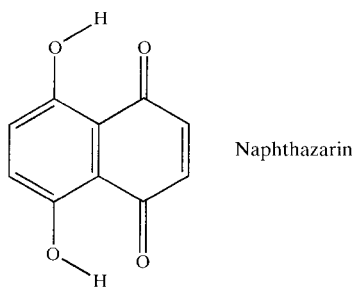

Naphthazarin (5,8-dihydroxy-1,4-naphthadione, polymorph *C*; Scheme 2) behaves quite differently, having a disorder-to-order phase transformation at 110 K (Herbstein *et al.*, 1985). The space group is $P2_1/c$ (Z = 4, two sets of molecules at independent centers of symmetry) down to 110 K, but Pc (Z = 4, no crystallographic requirement for molecular symmetry) below this temperature. The molecule is disordered above 110 K (no difference is discernible between the two C—O bonds; whether the disorder is static or dynamic is not known). The molecular arrangement becomes ordered below 110 K, following a classical Ising model; the difference between C—OH and C═O becomes more distinct as the temperature is lowered towards 0 K.

7. Relevance of present results to *cis*-enol systems in general

What sort of structural picture emerges from this investigation for benzoylacetone in particular and, by extension, for the family of *cis*-enols as a whole? We anticipate and remark that the structural picture appears to be unexpectedly diversified. We first summarize what has been found for the benzoylacetone molecule itself at 8 K. The phenyl and enol groups hardly librate mutually about the bond linking them, but the methyl group has a libration amplitude of ∼20° at 20 K and a larger (but unknown) amplitude at room temperature. We have concluded above that the *cis*-enol group has delocalized bonding between non-H atoms; in other words, there is an analogy to D_{6h} benzene, but not to the D_{3h} cyclohexatriene valence isomers. The enol hydrogen is in a large, flat-bottomed single potential well, a concept already used in the present context more than 25 years ago (Schlemper *et al.*, 1971).

Passing now to *cis*-enols as a group, we consider separately the two parameter relationships currently considered important in the analysis of geometrical effects in *cis*-enols. The first of these is the linear relationship found between q_2 (= $d_2 - d_3$) and q_1 (= $d_4 - d_1$; d_i defined in Scheme 1*a*). GBFB89 have presented such a plot, using the room-temperature dimensions of 20 *cis*-enol fragments as a database, and interpreted the linear relationship found in terms of the resonance-assisted model of (short) hydrogen bonds (RAHB), taking both intra- and intermolecular factors into account. Similar results, but with lower correlation factors, were obtained from a number of *cis*-enol crystal structures analyzed later (BGFG91). We have substantially extended the database for a fuller examination of the putative relationship, even though we have restricted ourselves to *cis*-enol systems (as shown in Scheme 1) with *intramolecular* hydrogen bonds. As we are not concerned with keto–enol tautomerism, R_3 can be H, C or S in order to cover information in the literature. Recourse to the Cambridge Structural Data File (CSD; Allen *et al.*, 1991) gives, after adding the conditions of error-free structures, not disordered, only organics, $R_F \leq 0.08$, and the enol ring not part of another ring system, around 40 structures (nine from BGFG91 and 34 not considered by them); a small number of the molecules included also have intermolecular hydrogen bonding. The details (numerical data and references) are given in Table Q. Apart from a few outliers, the linear dependence of q_2 on q_1 already reported by BGFG91 (their Fig. 2*a*) is confirmed (our Fig. 10). The examples near the upper right-hand corner of the diagram (q_1, $q_2 \simeq 0.10$ Å) are for molecules with *localized* C═O, C—O(H), C═C, C—C structures (such as acetylacetone; we have also used the term 'geometrically unsymmetrical'), while those near the lower left-hand corner (q_1, $q_2 \sim 0$ Å) are for delocalized structures (such as benzoylacetone; also called 'geometrically symmetrical') or for disordered structures (examples given below). The compounds between these extremes represent an unexplored region, which has not yet been analyzed in any depth. We now focus on some specific groups to assess the consistency and reliability of the geometrical information reported in the databases.

We first compare d_i values for the three polymorphs of dibenzoylmethane (Table 10; room-temperature studies). The sample s.u.s are appreciably larger than the experimental s.u.s, suggesting under-estimation of the latter (as is well known; Taylor & Kennard, 1986). The values of $q_i/u_{\rm sample}$ show that, despite the appearance of some bond alternation ($\langle q_1 \rangle = 0.017$, $\langle q_2 \rangle = 0.017$ Å), the

Table 10. *Bond lengths (Å) in the cis-enol ring of dibenzoylmethane at room temperature, as determined in its different polymorphs [(I), (II), (III)]*

All structures were determined at room temperature; the bond lengths have not been corrected for thermal motion. Calculation of q/u implicitly assumes that bond lengths do not differ among polymorphs.

Polymorph, method, reference	C1—O1	C2—O2	C1—C3	C2—C3	O1—H	O2—H	O1···O2
(I), XRD, (*a*)	1.277 (6)	1.302 (5)	1.404 (7)	1.377 (6)	1.34 (6)	1.18 (6)	2.460 (5)
(I), XRD, (*b*)	1.287 (2)	1.304 (2)	1.408 (3)	1.382 (2)	1.28 (3)	1.22 (3)	2.460 (2)
(I), ND, (*c*)	1.273 (4)	1.311 (4)	1.422 (3)	1.391 (3)	1.360 (9)	1.161 (9)	2.459 (4)
(II), XRD, (*d*)	1.294 (3)	1.299 (3)	1.387 (4)	1.383 (4)	1.28 (4)	1.22 (4)	2.452 (4)
(III), XRD, (*e*)	1.284 (3)	1.292 (3)	1.389 (4)	1.383 (4)	1.29†	1.26†	2.461 (4)
Unweighted mean [sample s.u.]	1.283 [8]	1.302 [7]	1.402 [14]	1.383 [5]	1.31 [4]	1.21 [4]	2.458 [4]
q/u (*f*)	0.019/0.011 = 1.73	0.019/0.015 = 1.27	0.10/0.06 = 1.67				

(*a*) Williams (1966); (*b*) Hollander *et al.* (1973); (*c*) Jones (1976*a*); (*d*) Etter *et al.* (1987); (*e*) Kaitner & Mestrovic (1993); (*f*) $q = |d_i - d_j|$; $u = [u(i)^2_{\text{sample}} + u(j)^2_{\text{sample}}]^{1/2}$. † S.u.s not given.

individual q_is do not differ significantly from zero. It is apparent that judicious inclusion (for possibly impeccable reasons) in the sample of only particular members [*e.g.* only the XRD studies of polymorphs (II) and (III)] can give an impression different from that obtained from the total available population. The (not very reliable) information about the enol H atoms for all three polymorphs favors single, almost symmetrically placed H atoms and thus chemically symmetrical dibenzoylmethane is presumed to have an ordered geometrically symmetrical structure in the solid state.

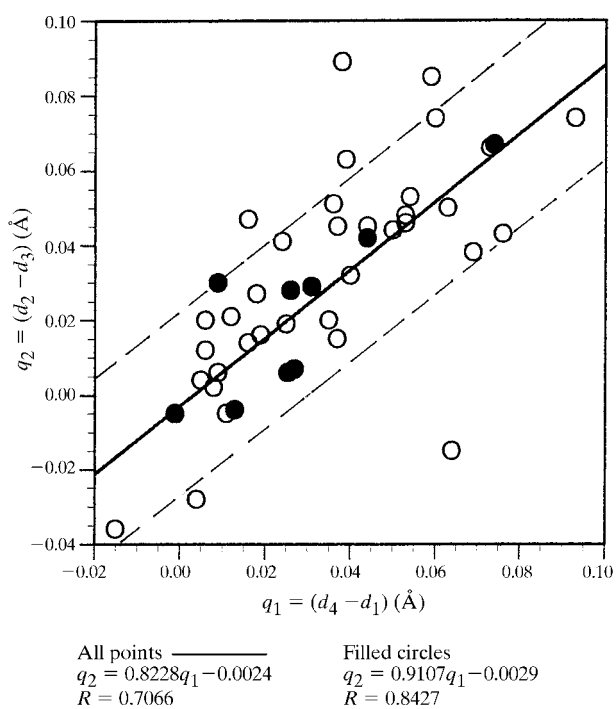

Fig. 10. Plot of q_2 (= $d_2 - d_3$) Å against q_1 (= $d_4 - d_1$) Å for the *cis*-enol data taken from the CSD. There are 34 data points (open circles) taken from the CSD (sources given in Table Q); the filled circles (9 points) are taken from BGFG91.

We next consider a group of closely related curcuminoid compounds (Table 11); we assume that the rather remote chemical substitution has little effect on the bond-length pattern in the *cis*-enol ring. PINHOJ and BUWKUZ have localized structures, as do (but less strongly) FAPLIR and COGWAW. YAPGUR (1,7-diphenyl-4-propenyl-1,6-heptadiene-3,5-dione; Görbitz & Mostad, 1993) crystallizes in space group $Cmc2_1$, Z = 4; T_{meas} = 121 K). The molecule has mirror symmetry [d(C—O) = 1.303 (2), d(C—C) = 1.413 (2), d(O···O) = 2.423 (2) Å] and two half-H atoms were found. The space group *Cmcm* would require *mm*2 molecular symmetry, which is not possible. An example where the molecule does not have imposed crystallographic symmetry (and is not symmetrical in the crystal because the 1,7 substituents are differently inclined to the *cis*-enol plane) is BINMEQ [1,7-bis(3′-methoxy-4′-hydroxyphenyl)-1,6-heptadiene-3,5-dione; Tønnesen *et al.*, 1982], which crystallizes in space group $P2/n$, Z = 4 at 121 K. Two positions were found for the enol hydrogen in the difference synthesis, even though the *cis*-enol ring is nearly symmetrical. Thus, the *cis*-enol ring appears to be disordered, despite the difference in the disposition of the 1,7 substituents. Thus, PINHOJ and BUWKUZ have ordered localized *cis*-enol ring structures, while in BINMEQ and YAPGUR the situation is the same as in acetylacetone at 110 K. FAPLIR and COGWAW lie in the central, unexplored region of Fig. 10. At the other extreme, CESMIW and FAPLEN have small values of q_1 and q_2, and both have a single, almost symmetrical location for the enol hydrogen. Thus, they appear to resemble benzoylacetone.

One other example of symmetry imposed exactly on a *cis*-enol ring by crystallographic considerations has been reported. The unit cell of bis(*m*-bromobenzoyl)methane contains four molecules and the *room-temperature* space group, *Pnca* [a non-standard setting of *Pbcn* (No. 60)], is unequivocally determined by the diffraction data (Williams *et al.*, 1962); the molecule has a twofold axis through the *cis*-enol ring. H atoms were inserted at calculated positions. Williams *et al.* (1962) concluded

that 'symmetry requires complete equivalence of the two C—O groups [d(C—O) = 1.306 (8) Å] and the intervening C—C bonds [d(C—C) = 1.393 (8) Å] of the enol ring, and the thermal parameters support the interpretation that this equivalence is real rather than statistical...All sensitive distances are more compatible with the [resonance] interpretation than any other'. It would be useful to repeat this structure analysis, especially at low temperatures, with the more powerful techniques currently available.

We summarize the results cited above as follows:

The curcuminoids BUWKUW and PINHOJ (Table 11) have ordered geometrically unsymmetrical (*i.e.* localized) molecular structures at 121 K. FAPLIR and COGWAW tend towards this situation.

Acetylacetone has an unsymmetrical molecular structure in the gas phase and in its 9-ethyladenine-diphenylhydantoin complex, but is disordered in its crystal (and hence *appears* to be symmetrical) down to (at least) 110 K; disorder in the crystal is also found for YAPGUR (1,7-diphenyl-4-propenyl-1,6-heptadiene-3,5-dione) and BINMEQ [1,7-bis(3′-methoxy,4′-hydroxyphenyl)-1,6-heptadiene-3,5-dione] at 121 K.

Benzoylacetone has a symmetrical geometrical structure at 8 K and its crystal structure does not change between 8 and 300 K, although there are undefined changes in the *cis*-enol ring starting somewhere between 20 and 140 K. Bis(*m*-bromobenzoyl)methane (at 300 K) has also been reported to have a (crystallographically) symmetrical structure; if intrinsically geometrically symmetrical (as is benzoylacetone) then a centered enol hydrogen should be found, otherwise two half-H atoms.

Naphthazarin (polymorph *C*) has an unsymmetrical molecular structure, which appears as such below 110 K; disordering occurs on heating above 110 K and the molecule *appears* to be symmetrical at higher temperatures.

Citrinin has two tautomeric forms, which impose valence isomerism, and is predominantly in the *o*-quinone form above 356 K and in the *p*-quinonemethide form below this temperature; despite this change in molecular structure the crystal structure does not change on cooling down to (at least) 19 K.

Having confirmed that there is a linear relation between q_2 and q_1 (the 'first' relationship proposed by the Gilli group), we now explore their 'second' proposal – that there is an approximately hyperbolic dependence of d_5 [= $d(O_1\cdots O_2)$] on Q (= $q_1 + q_2$). This is in line with the suggestion (Emsley, 1984; Emsley *et al.*, 1989) that there is a spectrum of *cis*-enol structures conveniently distinguished by the parameter d_5, which they have related to the form of the potential well in which the enol hydrogen is found. Q is plotted against d_5 for some 40-odd molecules in Fig. 11, in analogy to Fig. 2(*b*) of BGFG91. The appreciable scatter does not support any relation (linear or otherwise) between Q and d_5. Thus, consideration of the whole population of available results rather than a particular subset confirms the linear relation between q_2 and q_1, but does not show a correlation between Q and the non-bonded inter-oxygen distance (d_5). In assessing the validity of these conclusions one must take into account that the reported results, which cover a time scale of some 25 years, are perhaps less precise than one might have hoped (*cf.* dibenzoylmethane). Another possible factor is that the variety of chemical influences encountered here is considerably larger than that found for the group of closely similar compounds chosen for study by GBFB89 and BGFG91 and that their influence may be substantially greater than anticipated (*cf.* the curcuminoids).

Another parameter relationship worth exploring is that between the asymmetry of the enol hydrogen (expressed as $\{d(O_1\cdots H) - d(O_2\cdots H)\}$) and d_5. However, this would require accurate ND values for the position of the enol hydrogen and these are not available.

8. Theoretical calculations

Many of the earlier theoretical calculations on *cis*-enol systems have been reviewed by GBFB89. Bauer & Wilcox (1997) have recently considered whether theory and experiment are compatible for malonaldehyde and acetylacetone. For the latter, the complete basis set

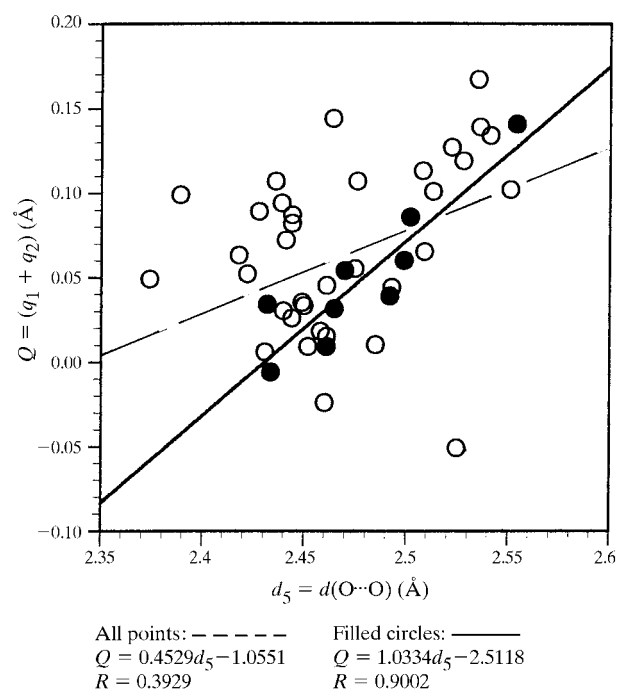

Fig. 11. Plot of Q (= $q_1 + q_2$) Å against $d_5 = d(O\cdots O)$ Å in *cis*-enols (see Scheme 2 for definition). There are 34 data points (open circles) taken from the CSD (sources given in Table Q); the filled circles (9 points) are taken from BGFG91.

Table 11. *Geometries of the cis-enol ring in various curcuminoids*

All structures were determined at 121 K, except for PINHOJ (293 K). Other information about some of these structures is given in §7. The compounds are ordered in terms of increasing localization (increasing Q).

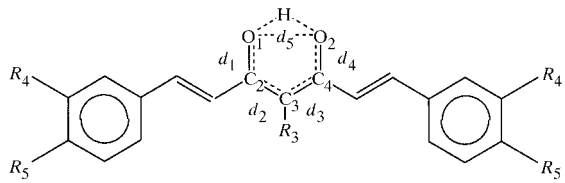

R_3	R_4	R_5	d_5 (Å)	$q_1 = d_4 - d_1$ (Å)	$q_2 = d_2 - d_3$ (Å)	$Q = q_1 + q_2$ (Å)	REFCODE/Reference
2-Oxy-2-ethoxy-ethyl	OCH_3	OH	2.432 (3)	0.010 (4)	−0.006 (6)	0.004 (7)	FAPLEN (*a*)
H	H	H	2.486 (6)	0.008 (7)	0.001 (7)	0.009 (10)	CESMIW (*b*)
H	OCH_3	OH	2.446 (2)	0.004 (3)	0.011 (4)	0.015 (5)	BINMEQ (*c*)
n-C_4H_9	H	H	2.442 (3)	0.040 (5)	0.031 (5)	0.071 (7)	COGWAW (*d*)
4-Benzyl	OCH_3	OCH_3	2.445 (2)	0.037 (3)	0.043 (3)	0.080 (4)	FAPLIR (*a*)
4-Benzyl	H	H	2.389 (7)	0.053 (11)	0.049 (13)	0.103 (16)	PINHOJ (*e*)
H	H	OH	2.514 (2)	0.054 (3)	0.049 (4)	0.103 (5)	BUWKUZ (*f*)
4-Propenyl	H	H	2.423 (2)	Molecular mirror plane			YAPGUR (*g*)

(*a*) Görbitz *et al.* (1986); intermolecular hydrogen bonding in FAPLEN, but not in FAPLIR. Both molecules have a single enol H, somewhat unsymmetrically located. (*b*) Mostad *et al.* (1983); single, almost symmetrical location for enol H. (*c*) Tønnesen *et al.* (1982); two half-H atoms in difference synthesis; intermolecular hydrogen bonding to both enol O atoms. (*d*) Mostad *et al.* (1984); single enol H, somewhat unsymmetrically located. (*e*) Mostad (1994); coordinates given for single enol H, but method of location unclear. (*f*) Tønnesen *et al.* (1983); methanol solvate; one enol oxygen participates in intermolecular hydrogen bonding; single, unsymmetrically located enol H. (*g*) Görbitz & Mostad (1993); molecule has crystallographic mirror plane; half hydrogen in difference synthesis.

method (CBS-4) of Ochterski *et al.* (1996) (incorporated in the *Gaussian*94, Revision B.2, program package; Frisch *et al.*, 1995) was used to calculate $\Delta U(C_{2v} - C_s)$ (= 12 kJ mol^{-1}), $\Delta E(C_{2v} - C_s)$ (0 K) (= 1.7 kJ mol^{-1}) and $\Delta H(C_{2v} - C_s)$ (298 K; = 0.4 kJ mol^{-1}), where C_{2v} represents the symmetrical structure (the resonance structure 1*e* in Scheme 1) and C_s the unsymmetrical structure (tautomers *A* and *B* in Scheme 1). Thus, the unsymmetrical structure is slightly favored, in agreement with the earlier MP2/D95++** level calculations of Dannenberg & Rios (1994), but the relative energies of the two species are such that comparable populations would be expected in the gas phase at 300 K. Instead, FTIR spectroscopy shows only 'a single, well assigned set of absorption bands and not a superposition of two distinct patterns'. There is agreement between the FTIR and electron diffraction results, but these do not agree with the calculations.

B3LYP/6-311G(d,p) level calculations for benzoylacetone (Schiøtt *et al.*, 1998) give results essentially similar to those obtained by analogous techniques for acetylacetone, but there are non-negligible differences between those calculations and the experimental results given here. The calculation gives an unsymmetrical structure for a separation of ∼2.5 Å between nonbonded O atoms and a symmetrical transition-state structure when this separation is reduced to 2.359 Å. It is, of course, well known that very strong symmetrical hydrogen bonds are only found when $d(O\cdots O)$ is less than 2.4 Å. The disagreement between theory and experiment arises from the fact that, experimentally, we find a symmetrical structure when $d(O\cdots O) \simeq 2.5$ Å. There appears to be a compatibility problem similar to that pointed out by Bauer & Wilcox (1997) for acetylacetone. One interesting feature of the Schiott calculations is the (one-dimensional) potential energy surface obtained for the methyl–enol/phenyl–enol pair (their Fig. 3). The energies of both ^{1}H and ^{2}H benzoylacetone lie well above the surface, suggesting that the two molecules should have very similar structures. Emsley (1984) has advanced the possibility that the deuterated compound could be located below the potential barrier, whereas the hydrogenated compound could lie well above, thus leading to a symmetrical structure for the hydrogenated compound and an unsymmetrical one for the deuterated compound. This possible difference between ^{1}H and ^{2}H benzoylacetone is not supported by the Schiott calculations.

9. Other techniques which have been or could be used

There are other potential sources of independent information about the structures of *cis*-enols. These include solution and solid-state NMR studies, matrix isolation Fourier transform IR spectroscopy, inelastic neutron spectroscopy and specific heat measurements. As the information currently available is somewhat inconclusive, we have deposited this material (with references).

Table 12. *Tentative assignment of some compounds to structure types (references in the text); complete coverage has not been attempted*

Ordered localized (geometrically unsymmetrical) structures	**Disordered localized (geometrically unsymmetrical) structures**
4-Benzyl-1,7-diphenyl-1,6-heptadiene-3,5-dione (PINHOJ)	Acetylacetone
	1,7-Diphenyl-4-propenyl-1,6-heptadiene-3,5-dione (YAPGUR)
1,7-Bis(4-hydroxyphenyl)-1,6-heptadiene-3,5-dione (BUKWUZ)	
	1,7-Bis(3′-methoxy-4′-hydroxyphenyl)-1,6-heptadiene-3,5-dione (BINMEQ)
Ordered delocalized (geometrically symmetrical) structures	**Unexplored intermediate region**
Benzoylacetone	
	1,7-Bis(4-hydroxy-3-methoxyphenyl)-1,6-heptadiene-3,5-dione (FAPLIR; curcumin)
Dibenzoylmethane (all three polymorphs)	
	4-Butyl-1,7-diphenyl-1,6-heptadiene-3,5-dione (COGWAW)
Bis(*m*-bromobenzoyl)methane; 1,7-diphenyl-1,6-heptadiene-3,5-dione (CESMIW)	

10. Conclusions

10.1. *Diffraction studies of the benzoylacetone crystal and molecule*

Diffraction studies (mainly XRD) indicate that the overall crystal structure of benzoylacetone does not change appreciably over the range 8–300 K and show that, pairwise, the two C—C and the two C–O bonds of the enol ring do not differ significantly in length. The 20 K ND difference-synthesis evidence of a single position for the enol hydrogen, albeit with a large vibration amplitude of ~0.30 Å along the O···O direction, appears to show that the symmetry of the enol ring arises from a single π-delocalized structure rather than from the superpositioning of two localized structures. There is no diffraction evidence for static or dynamic disorder of the phenyl ring in crystalline benzoylacetone up to, at least, 160 K. The situation of the *cis*-enol rings is more complicated. The 8 K XRD study supports a single delocalized structure at this temperature, while at higher temperatures the *cis*-enol ring is less rigid, although we have not been able to define this in structural terms. At 8–20 K the enol hydrogen is in a broad single-minimum potential well; this is case 3 of Emsley's (1984) classification of *cis*-enol potential wells.

10.2. *Other types of study*

According to high-level computations, the energy difference between the single- and double-minimum potential well models is less than 1 kJ mol^{-1} in acetylacetone and benzoylacetone. The double well is the more stable until the zero-point energy, which essentially nullifies the difference, is included. Bauer & Wilcox (1997) have pointed out that experiment and theory have not yet reached compatibility for *cis*-enols and our present results support this point of view.

Distinction between the pairs of quasi-equivalent C atoms and O atoms in the *cis*-enol ring of benzoylacetone has been attempted *via* solution and solid-state ^{13}C and solution ^{17}O NMR studies; matrix-isolation IR spectroscopy possibly shows similar effects. Details of the as-yet somewhat inconclusive NMR and IR studies have been deposited.

10.3. *Survey of interatomic distances in cis-enol systems*

A survey of all the relevant *cis*-enol systems for which diffraction results have been reported shows a correlation between q_1 (= $d_1 - d_4$) and q_2 (= $d_2 - d_3$). The correlation between d(O···O) and the degree of localization of the quasi-equivalent C—C and C—O bond pairs [the longer d(O···O) the more definite the distinction between single and double bonds, and *vice versa*] has not been confirmed using a database more extensive than that employed in earlier studies.

10.4. *Paradoxical inverse relation between structural completeness and chemical relevance*

The most detailed information about the structure of the *cis*-enol ring in benzoylacetone has been obtained from diffraction studies made at the lowest temperatures attainable (8 and 20 K). Above these temperatures conformational versatility (which we have not been able to define) sets in and our knowledge of the structure is considerably reduced. This difference does not apply to the phenyl ring; our knowledge of its structure is only marginally less at 300 K than at 20 K. Of course, chemists are far more interested in behavior (and in understanding behavior through a detailed knowledge of structure) at 300 K (or above) than at 20 K or below.

Thus, we have the paradoxical situation that we know most about the *cis*-enol ring at temperatures where such knowledge is least useful in a chemical sense.

10.5. *Implications of the present study: the electronic structure of the benzoylacetone molecule*

Geometrically unsymmetrical *cis*-enols (localized single and double C—C and C—O bonds) can be characterized without undue difficulty when the crystal structure is ordered. The problems arise when the diffraction analysis shows the *cis*-enol ring to be symmetrical – are we seeing a truly delocalized structure, as appears to be the situation in crystalline benzoylacetone and a few other examples, or the disordered superpositioning of two unsymmetrical structures, as in crystalline acetylacetone above 110 K? The distinction could be made by determination of the location of the enol hydrogen (single or double position) or, possibly, by using the Hirshfeld displacement analysis. Most of the published diffraction results are not precise enough to allow these tests, nor do ^{13}C NMR results provide a recipe for distinguishing between the two situations. Our study suggests that this delicate distinction may best be made by low-temperature ND (location of enol hydrogen); XRD may be satisfactory for this task if crystal quality is adequate. Hirshfeld analysis based on low-temperature XRD may be an additional method, but our present measurements were not precise enough to demonstrate this.

We have substantiated that the benzoylacetone crystal structure is ordered and that the H atom in the keto–enol group is located slightly unsymmetrically in a broad single-potential well; there are also strong indications that the *cis*-enol ring is π-delocalized. These findings were crucial for carrying out (in the related paper by Madsen *et al.*, 1998) a full multipolar refinement and detailed topological analysis of the charge density of the benzoylacetone molecule. High formal charges were found on both the O atoms and the enol hydrogen and it was concluded that the bonding of the hydrogen in the short, almost symmetrical intramolecular O—H—O hydrogen bond in benzoylacetone at each side of the hydrogen has partly covalent and partly electrostatic contributions.

Finally, we give a molecular (localized or delocalized) and crystal (ordered or disordered) classification of some *cis*-enol structures in Table 12.

We are grateful to Professor J. D. Dunitz and three anonymous referees for penetrating and helpful comments. Principal financial support for the project at Technion came from the US–Israel Binational Science Foundation, the Fund of the Vice-president for Research and the Fund for the Promotion of Research, while the Israel–Denmark Scientific Exchange Programme helped to make Dr Reisner's participation in some of the Aarhus measurements possible. The Carlsberg Foundation is acknowledged for the low-temperature X-ray diffractometer in Aarhus. GKHM thanks Aarhus University for financial support. We are grateful to many colleagues for helpful discussions and, particularly, to Professor Roland Boese (Essen) for advance information about acetylacetone, and to Professor Hans-Beat Bürgi (Bern) for emphasizing the importance of multiple-temperature measurements.

References

Albertsson, J., Oskarsson, Å., Ståhl, K., Svensson, C. & Ymén, I. (1980). *Acta Cryst.* B**36**, 3072–3078.
Allen, F. H., Davies, J. E., Galloy, J. J., Johnson, O., Kennard, O., Macrae, C. F., Mitchell, E. M., Mitchell, G. F., Smith, J. M. & Watson, D. G. (1991). *J. Chem. Inf. Comput. Sci.* **31**, 187–204.
Bader, R. F. W. (1990). *Atoms in Molecules. A Quantum Theory*. Oxford University Press.
Bauer, S. H. & Wilcox, C. F. (1997). *Chem. Phys. Lett.* **279**, 122–128.
Becker, P. & Coppens, P. (1974). *Acta Cryst.* A**30**, 129–147.
Bertolasi, V., Gilli, P., Ferretti, V. & Gilli, G. (1991). *J. Am. Chem. Soc.* **113**, 4917–4925.
Bertolasi, V., Gilli, P., Ferretti, V. & Gilli, G. (1996). *Chem. Eur. J.* pp. 925–934.
Bertolasi, V., Gilli, P., Ferretti, V. & Gilli, G. (1997). *J. Chem. Soc. Perkin Trans. 2*, pp. 945–952.
Blessing, R. H. (1989). *J. Appl. Cryst.* **22**, 396–397.
Boese, R., Antipin, M. Yu., Bläser, D. & Lyssenko, K. A. (1998). *J. Phys. Chem. B*, **102**, 8654–8660.
Brock, C. P. & Dunitz, J. D. (1982). *Acta Cryst.* B**38**, 2218–2228.
Brock, C. P. & Dunitz, J. D. (1990). *Acta Cryst.* B**46**, 795–806.
Brock, C. P., Schweitzer, W. B. & Dunitz, J. D. (1985). *J. Am. Chem. Soc.* **107**, 6964–6970.
Bürgi, H.-B. & Förtsch, M. (1997). Abstract P2.7-13, ECM-17. Lisbon, Portugal.
Camerman, A., Mastropaolo, D. & Camerman, N. (1983). *J. Am. Chem. Soc.* **105**, 1584–1586.
Chandrasekhar, K. & Bürgi, H.-B. (1984). *Acta Cryst.* B**40**, 387–397.
Clementi, E. & Roetti, C. (1974). *At. Nucl. Data Tables*, **14**, 177–478.
Coppens, P., Leiserowitz, L. & Rabinovich, D. (1965). *Acta Cryst.* **18**, 1035–1038.
Dannenberg, J. J. & Rios, R. (1994). *J. Phys. Chem.* **98**, 6714–6718.
Destro, R. (1991). *Chem. Phys. Lett.* **181**, 232–236.
Destro, R. & Marsh, R. E. (1984). *J. Am. Chem. Soc.* **106**, 7269–7271.
Destro, R., Marsh, R. E. & Bianchi, R. (1988). *J. Phys. Chem.* **92**, 966–973.
Dunitz, J. D. (1979). *X-ray Analysis and the Structure of Organic Molecules*, pp. 244–261. Ithaca: Cornell University Press (1995 reprint by *Helv. Chim. Acta*, Basel).
Dunitz, J. D., Krüger, C., Irngartinger, H., Maverick, E. F., Wang, Y. & Nixdorf, M. (1988). *Angew. Chem. Int. Ed. Engl.* **27**, 387–389.
Dunitz, J. D., Maverick, E. F. & Trueblood, K. N. (1988). *Angew. Chem. Int. Ed. Engl.* **27**, 880–895.

Dunitz, J. D., Schomaker, V. & Trueblood, K. N. (1988). *J. Phys. Chem.* **92**, 856–867.
Emsley, J. (1984). *Struct. Bonding (Berlin)*, **57**, 147–191.
Emsley, J., Ma, L. Y. Y., Bates, P. A., Motevalli, M. & Hursthouse, M. B. (1989). *J. Chem. Soc. Perkin Trans. II*, pp. 527–533.
Ermer, O. (1987). *Angew. Chem. Int. Ed. Engl.* **26**, 782–784.
Etter, M. A., Jahn, D. A. & Urbanczyk-Lipkowska, Z. (1987). *Acta Cryst.* C**43**, 260–263.
Fischer, R. X. & Tillmanns, E. (1988). *Acta Cryst.* C**44**, 775–776.
Frisch, M. J., Trucks, G. W., Schlegel, H. B., Gill, P. M. W., Johnson, B. G., Robb, M. A., Cheeseman, J. R., Keith, T., Peterson, G. A., Montgomery, J. A., Raghavachari, K., Al-Laham, M. A., Zakrzewski, V. G., Ortiz, J. V., Foresman, J. B., Peng, C. Y., Ayala, P. Y., Chen. W., Wong, M. W., Andres, J. L., Replogle, E. S., Gomperts, R., Martin, R. L., Fox, D. J., Binkley, J. S., DeFrees, D. J., Baker, J., Stewart, J. D., Head-Gordon, M., Gonzalez, C. & Pople, J. A. (1995). *Gaussian*94, Revision B.2. Gaussian Inc., Pittsburgh PA, USA.
Gilli, G., Bellucci, F., Ferretti, V. & Bertolasi, V. (1989). *J. Am. Chem. Soc.* **111**, 1023–1028.
Gilli, P., Ferretti, V. & Gilli, G. (1996). *Fundamental Principles of Molecular Modelling*, edited by W. Gans, A. Amann & J. C. A. Boeyens, pp. 119–141. New York: Plenum Press.
Görbitz, C. H. & Mostad, A. (1993). *Acta Chem. Scand.* **47**, 509–513.
Görbitz, C. H., Mostad, A., Pedersen, U., Rasmussen, P. B. & Lawesson, S.-O. (1986). *Acta Chem. Scand. B*, **40**, 420–429.
Hansen, N. K. & Coppens, P. (1978). *Acta Cryst.* A**34**, 904–921.
Hazell, A. C. (1995). *KRYSTAL. An Integrated System of Crystallographic Programs*. University of Aarhus, Denmark.
Henriksen, K., Larsen, F. K. & Rasmussen, S. E. (1986). *J. Appl. Cryst.* **19**, 390–394.
Herbstein, F. H., Borie, B. S. Jr & Averbach, B. L. (1956). *Acta Cryst.* **9**, 466–471.
Herbstein, F. H., Kapon, M., Reisner, G. M., Lehmann, M. S., Kress, R. B., Wilson, R. B., Shiau, W.-I., Duesler, E. N., Paul, I. C. & Curtin, D. Y. (1985). *Proc. R. Soc. London A*, **399**, 295–319.
Hibbert, F. & Emsley, J. (1990). *Adv. Phys. Org. Chem.* **26**, 255–379.
Hirshfeld, F. L. (1976). *Acta Cryst.* A**32**, 239–244.
Hollander, F. J., Templeton, D. H. & Zalkin, A. (1973). *Acta Cryst.* B**29**, 1552–1553.
Howard, J. A. K., Johnson, O., Schulz, A. J. & Stringer, A. M. (1989). *J. Appl. Cryst.* **20**, 120–122.
Huang, K. (1947). *Proc. R. Soc. London A*, **190**, 102–117.
Iijima, K., Ohnogi, A. & Shibata, S. (1987). *J. Mol. Struct.* **156**, 111–118.
James, R. W. (1948). *Acta Cryst.* **1**, 132–134.
Johnson, C. K. (1976). Report ORNL-3794. Oak Ridge National Laboratory, Oak Ridge, Tennessee, USA.
Jones, R. D. G. (1976*a*). *Acta Cryst.* B**32**, 1807–1811.
Jones, R. D. G. (1976*b*). *Acta Cryst.* B**32**, 2133–2136.
Kaitner, B. & Mestrovic, E. (1993). *Acta Cryst.* C**49**, 1523–1525.
Koritsanszky, T. (1996). *Fundamental Principles of Molecular Modelling*, edited by W. Gans, A. Amann & J. C. A. Boeyens, pp. 143–166. New York: Plenum Press.
Koritsanszky, T., Howard, S., Mallinson, P. R., Su, Z., Richter, T. & Hansen, N. K. (1995). *XD. A Computer Program Package for Multipole Refinement and Analysis of Charge Densities from Diffraction Data*. Institute of Crystallography, Free University, Berlin, Germany.
Lehmann, M. S. & Larsen, F. K. (1974). *Acta Cryst.* A**30**, 580–584.
Le Page, Y. & Gabe, E. J. (1979). *Acta Cryst.* A**35**, 73–78.
Madsen, G. K. H., Iversen, B. B., Larsen, F. K., Kapon, M., Reisner, G. M. & Herbstein, F. H. (1998). *J. Am. Chem. Soc.* **120**, 10040–10045.
Marsh, R. E. (1986). *Acta Cryst.* B**42**, 193–198.
Maverick, E. M. & Dunitz, J. D. (1987). *Mol. Phys.* **62**, 451–459.
Mostad, A. (1994). *Acta Chem. Scand.* **48**, 144–148.
Mostad, A., Pedersen, U., Rasmussen, P. B. & Lawesson, S.-O. (1983). *Acta Chem. Scand. B*, **37**, 901–905.
Mostad, A., Pedersen, U., Rasmussen, P. B. & Lawesson, S.-O. (1984). *Acta Chem. Scand. B*, **38**, 479–484.
Ochterski, J. W., Petersson, G. A. & Montgomery, J. A. Jr (1996). *J. Chem. Phys.* **104**, 2598–2619.
Perrin, C. L. & Kim, Y.-J. (1998). *J. Am. Chem. Soc.* **120**, 12641–12645.
Poupko, R., Luz, Z. & Destro, R. (1997). *J. Phys. Chem. A*, **101**, 5097–5102.
Roversi, P., Barzaghi, M., Merati, F. & Destro, R. (1996). *Can. J. Chem.* **74**, 1145–1161.
Schiøtt, B., Iversen, B. B., Madsen, G. K. H. & Bruice, T. H. (1998). *J. Am. Chem. Soc.* **120**, 12117–12124.
Schlemper, E. O., Hamilton, W. C. & La Placa, S. J. (1971). *J. Chem. Phys.* **54**, 3990–4000.
Schomaker, V. & Marsh, R. E. (1983). *Acta Cryst.* A**39**, 819–820.
Schomaker, V. & Trueblood, K. N. (1968). *Acta Cryst.* B**24**, 63–76.
Sears, V. F. (1992). *Neutron News*, **3**, 26–37.
Semmingsen, D. (1972). *Acta Chem. Scand.* **26**, 143–154.
Semmingsen, D. (1977). *Acta Chem. Scand. B*, **31**, 114–118.
Sequeira, A., Berkebile, C. A. & Hamilton, W. C. (1968). *J. Mol. Struct.* **1**, 283–294.
Stewart, R. F. (1973). *J. Chem. Phys.* **58**, 1668–1676.
Stewart, R. F. (1991). *The Application of Charge Density Research to Chemistry and Drug Design*, edited by G. A. Jeffrey and J. F. Piniella, pp. 63–101. New York: Plenum Press.
Taylor, R. & Kennard, O. (1986). *Acta Cryst.* B**42**, 112–120.
Tønnesen, H. H., Karlsen, J. & Mostad, A. (1982). *Acta Chem. Scand. B*, **36**, 475–479.
Tønnesen, H. H., Karlsen, J., Mostad, A., Pedersen, U., Rasmussen, P. B. & Lawesson, S.-O. (1983). *Acta Chem. Scand. B*, **37**, 179–185.
Trueblood, K. N. (1978). *Acta Cryst.* A**34**, 950–954.
Vila, A. J., Lagier, C. M. & Olivieri, A. C. (1992). *J. Mol. Struct.* **274**, 215–222.
Williams, D. E. (1966). *Acta Cryst.* **21**, 340–349.
Williams, D. E., Dumke, W. L. & Rundle, R. E. (1962). *Acta Cryst.* **15**, 627–635.
Winter, W., Zeller, K. P. & Berger, S. (1979). *Z. Naturforsch. Teil B*, **34**, 1606–1611.